



Original Article

# Non-autophagy Role of Atg5 and NBR1 in Unconventional Secretion of IL-12 Prevents Gut Dysbiosis and Inflammation

Seth D. Merkle<sup>a,#</sup>, Samuel M. Goodfellow<sup>b,#</sup>, Yan Guo<sup>a</sup>, Zoe E. R. Wilton<sup>a</sup>,  
Janie R. Byrum<sup>c</sup>, Kurt C. Schwalm<sup>d</sup>, Darrell L. Dinwiddie<sup>d,e</sup>,  
Rama R. Gullapalli<sup>f</sup>, Vojo Deretic<sup>c,g</sup>, Anthony Jimenez Hernandez<sup>a</sup>,  
Steven B. Bradfute<sup>b,e</sup>, Julie G. In<sup>a,h</sup>, Eliseo F. Castillo<sup>a,e,g,e</sup>

<sup>a</sup>Division of Gastroenterology and Hepatology, Department of Internal Medicine, University of New Mexico Health Sciences, Albuquerque, NM, USA <sup>b</sup>Center for Global Health, Department of Internal Medicine, University of New Mexico Health Sciences, Albuquerque, NM, USA <sup>c</sup>Department of Molecular Genetics and Microbiology, University of New Mexico Health Sciences, Albuquerque, NM, USA <sup>d</sup>Department of Pediatrics, University of New Mexico Health Sciences, Albuquerque, NM, USA <sup>e</sup>Clinical and Translational Science Center, University of New Mexico Health Sciences, Albuquerque, NM, USA <sup>f</sup>Department of Pathology, University of New Mexico Health Sciences, Albuquerque, NM, USA <sup>g</sup>Autophagy Inflammation and Metabolism Center of Biomedical Research Excellence, University of New Mexico Health Sciences, Albuquerque, NM, USA <sup>h</sup>Division of Gastroenterology and Hepatology, Department of Medicine, Johns Hopkins University School of Medicine, Baltimore, MD, USA

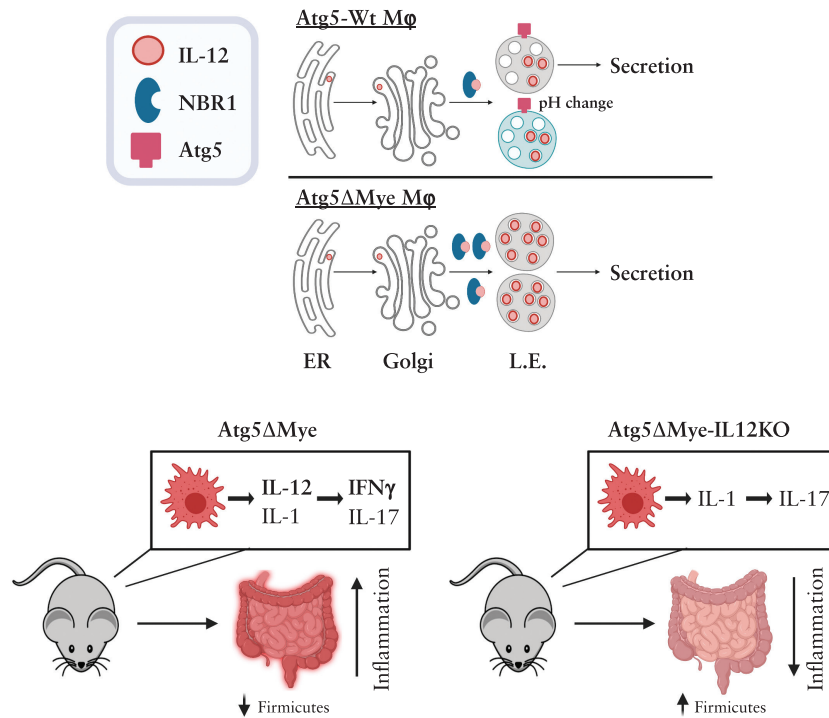
Corresponding author: Eliseo F. Castillo, PhD, Department of Internal Medicine, MSC 10 550, 1 University of New Mexico, Albuquerque, New Mexico 87131, USA. Email: [ecastillo@salud.unm.edu](mailto:ecastillo@salud.unm.edu)

<sup>#</sup>Authors contributed equally to this study.

## Abstract

Intestinal myeloid cells play a critical role in balancing intestinal homeostasis and inflammation. Here, we report that expression of the autophagy-related 5 [Atg5] protein in myeloid cells prevents dysbiosis and excessive intestinal inflammation by limiting IL-12 production. Mice with a selective genetic deletion of *Atg5* in myeloid cells [Atg5 $\Delta$ Mye] showed signs of dysbiosis preceding colitis, and exhibited severe intestinal inflammation upon colitis induction that was characterised by increased IFN $\gamma$  production. The exacerbated colitis was linked to excess IL-12 secretion from *Atg5*-deficient myeloid cells and gut dysbiosis. Restoration of the intestinal microbiota or genetic deletion of IL-12 in Atg5 $\Delta$ Mye mice attenuated the intestinal inflammation in Atg5 $\Delta$ Mye mice. Additionally, Atg5 functions to limit IL-12 secretion through modulation of late endosome [LE] acidity. Last, the autophagy cargo receptor NBR1, which accumulates in Atg5-deficient cells, played a role by delivering IL-12 to LE. In summary, Atg5 expression in intestinal myeloid cells acts as an anti-inflammatory brake to regulate IL-12, thus preventing dysbiosis and uncontrolled IFN $\gamma$ -driven intestinal inflammation.

## Graphical abstract



**Key Words:** Autophagy; macrophages; inflammation; cytokines; microbiota

## 1. Introduction

Immune system dysregulation, intestinal barrier defects, and dysbiosis are believed to be driven in part by genetics, according to recent genome-wide association studies [GWAS].<sup>1</sup> Many of the identified genes are involved in innate cell bacterial recognition and processing, and appear to contribute to the pathogenesis observed in inflammatory bowel disease [IBD], such as *NOD2* and *ATG16L1* which are linked to autophagy.<sup>1</sup> Autophagy is one such process associated with IBD susceptibility.<sup>2–11</sup> Autophagy is a conserved catabolic process that degrades protein aggregates, damaged organelles, and numerous pathogens.<sup>12</sup> Autophagy has proven critical for intestinal homeostasis. Defects in the autophagic pathway, specifically in intestinal epithelial cell lineages, results in increased intestinal permeability and Paneth and goblet cell [GC] dysfunction.<sup>13–18</sup> More recently, an IBD risk locus associated with autophagy was found to disrupt the microbiota, albeit it is unclear what cell type mediates this effect.<sup>19</sup> Nevertheless, there is mounting evidence that autophagic genes are critical for intestinal homeostasis, and defects in the autophagic process can lead to increased susceptibility to intestinal pathogens and overall enhanced IBD susceptibility.<sup>6,20–22</sup>

Many of these IBD risk genes and pathways, including autophagy, are highly relevant to myeloid cell function in addition to that of epithelial cells.<sup>23–26</sup> However, the specific role for autophagy and autophagy genes in myeloid cells in maintaining the balance between intestinal homeostasis and inflammation has yet to be fully explored. The prevailing hypothesis linking autophagy to IBD is through the IL-17 signalling pathway. IL-1, IL-17, and IL-23, all involved in IL-17-mediated inflammation, are upregulated in IBD.<sup>27–36</sup> Our previous work, as well as that of others, has demonstrated that

autophagy regulates the production of the proinflammatory cytokines IL-1 $\alpha$ , IL-1 $\beta$ , and IL-23, primarily in infection models.<sup>37–42</sup> This observation is the canonical pathway frequently described linking autophagy dysregulation to excess inflammation via IL-1 and IL-17. IL-1 and IL-23 are key regulators of IL-17-mediated inflammation.<sup>43,44</sup> However, the role of IL-17 in IBD pathogenesis has recently been questioned, as therapeutic targeting of IL-17 exacerbates inflammation in both IBD patients and animal models of IBD,<sup>45–49</sup> suggesting that IL-17 may not be the predominant driver of autophagy-linked IBD pathogenesis. Thus, there is a clear gap in knowledge regarding which inflammatory pathway might underlie IBD pathology with respect to autophagy dysregulation.

This study assessed the role of the autophagy gene *Atg5* in myeloid cells in maintaining the balance between intestinal homeostasis and inflammation. *Atg5*'s most well-understood actions are via the *Atg5-Atg12-Atg16L1* complex, which acts as the E3 enzyme conjugating PE to LC3, and along with the E1-like actions of *Atg7* and the E2-like actions of *Atg3*, this pathway drives isolation membrane formation and eventual autophagosome maturation.<sup>50–53</sup> *Atg5* is also embedded in autophagosomal membranes, which allows it to interact with fusion proteins in lysosomal membranes such as Tectonic  $\beta$ -propeller repeat containing 1 [TECRP] that facilitate autophagosome-lysosome fusion.<sup>54,55</sup> Thus, *Atg5* plays a major role in selective and bulk autophagy which are critical for cell autonomous immunity. However, it is unclear how *Atg5* expression, specifically in myeloid cells, functions outside of bacterial recognition and processing. Here, we show at steady state that mice with an *Atg5*-deficiency in myeloid cells [herein called *Atg5ΔMye* mice]<sup>37,56</sup> show alterations in the gut microbiota as well as mucosal TH1 [IFN $\gamma$ ]

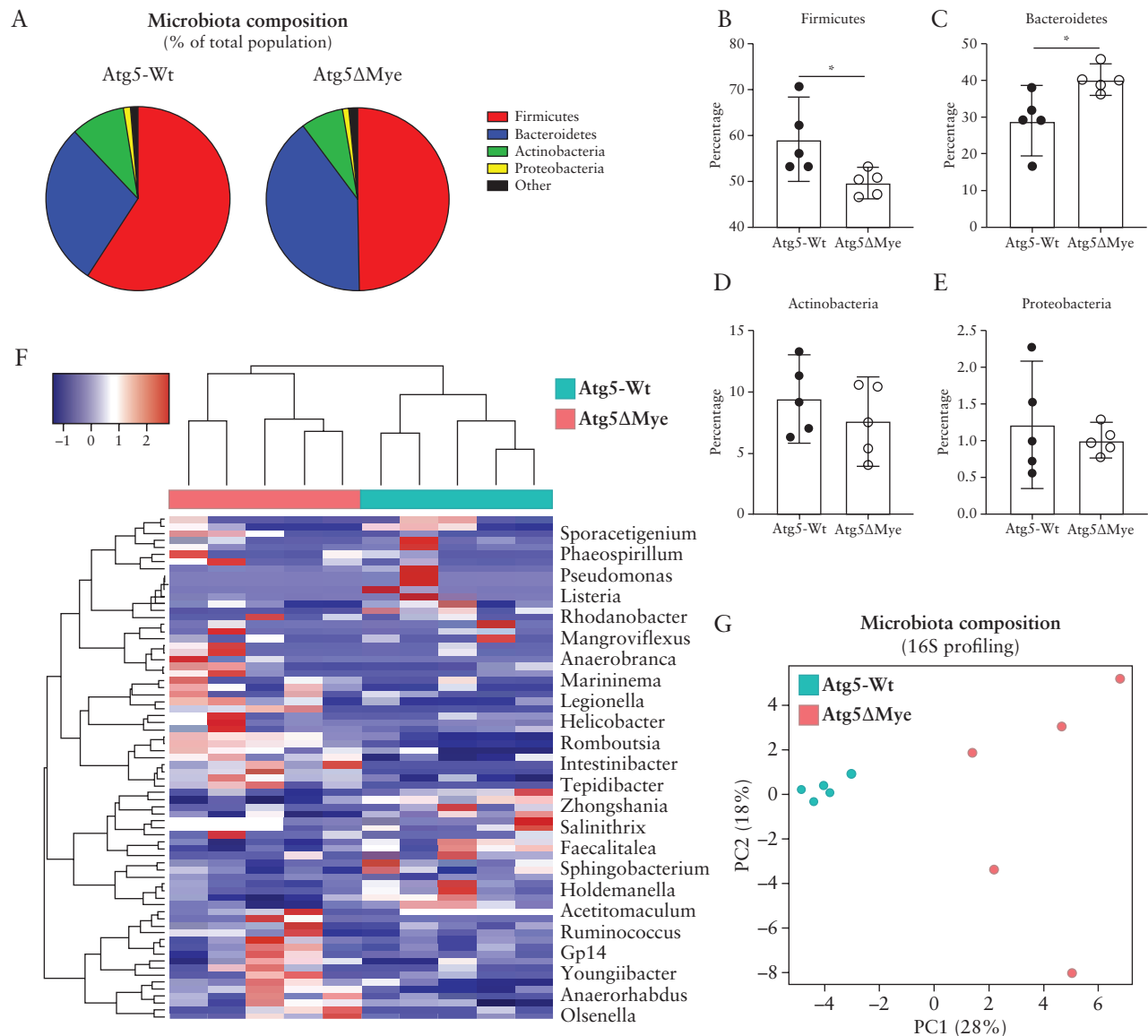


**Figure 1.** Alterations in the composition of the colonic microbial community in mice with a selective *Atg5*-deficiency in myeloid cells. Bacterial composition as assessed by 16S rRNA sequencing of DNA extracted from freshly collected stool of *Atg5*-Wt and *Atg5*ΔMyc mice ( $n = 5$  per group). [A] Pie chart showing the average proportion of Firmicutes, Bacteroidetes, Actinobacteria, Proteobacteria, and all other phyla in 8-week old mice. [B-E] Quantification of the phyla [B] Firmicutes, [C] Bacteroidetes, [D] Actinobacteria, and [E] Proteobacteria. [F] Heatmap of the relative abundance of colonic microbes [genus level]. [G] Principal coordinates analysis [PCoA] plot of microbiota composition [genus level]. Data are shown as mean ( $\pm 95\%$  confidence interval [CI]) and a t test was used to measure specific microbiome species abundance between groups. Adjusted  $p$ -value  $>0.05$  was used as significant threshold.

skewing. *Atg5*ΔMyc mice were susceptible to chemically-induced colitis that was characterised by an enhanced  $\text{IFN}\gamma$  response. Both TH1 skewing and microbiota changes were partly driven through IL-12 dysregulation in *Atg5*-deficient myeloid cells. Confirming our findings, *Atg5*ΔMyc mice crossed with *IL12p35*-deficient mice resulted in restoration of the gut microbiota and protection from dextran sodium sulphate [DSS]-induced colitis through the reduction of the IL-12 pathway. In addition, faecal microbiota transplant of control microbiota into *Atg5*ΔMyc mice reduced chemically-induced colitis, suggesting the *Atg5*ΔMyc-associated microbiota also contributes to the exacerbated colitis phenotype in *Atg5*ΔMyc mice. We further show IL-12 regulation was not mediated through autophagy but through interactions with sequestosome-1-like receptor NBR1 and *Atg5* action on late endosomes [LE]. There has not been a single description of autophagic proteins regulating IL-12-driven immune

responses. Thus, these data indicate a new autophagy-independent role for *Atg5* and NBR1 in myeloid cells in influencing intestinal homeostasis through an IL-12 pathway.

## 2. Results

### 2.1. Altered colonic microbiota in mice with an *Atg5*-deficiency in myeloid cells

The gut microbiota is influenced by environmental factors, immune responses, and genetics which is highlighted in individuals with IBD. Numerous studies have reported a decrease in bacterial diversity in IBD patients, with major alterations in the phyla Firmicutes and Bacteroidetes.<sup>57-62</sup> There is substantial evidence that intestinal myeloid cells are regulated by commensal microbiota.<sup>58,63-66</sup> However, numerous studies have emerged demonstrating myeloid

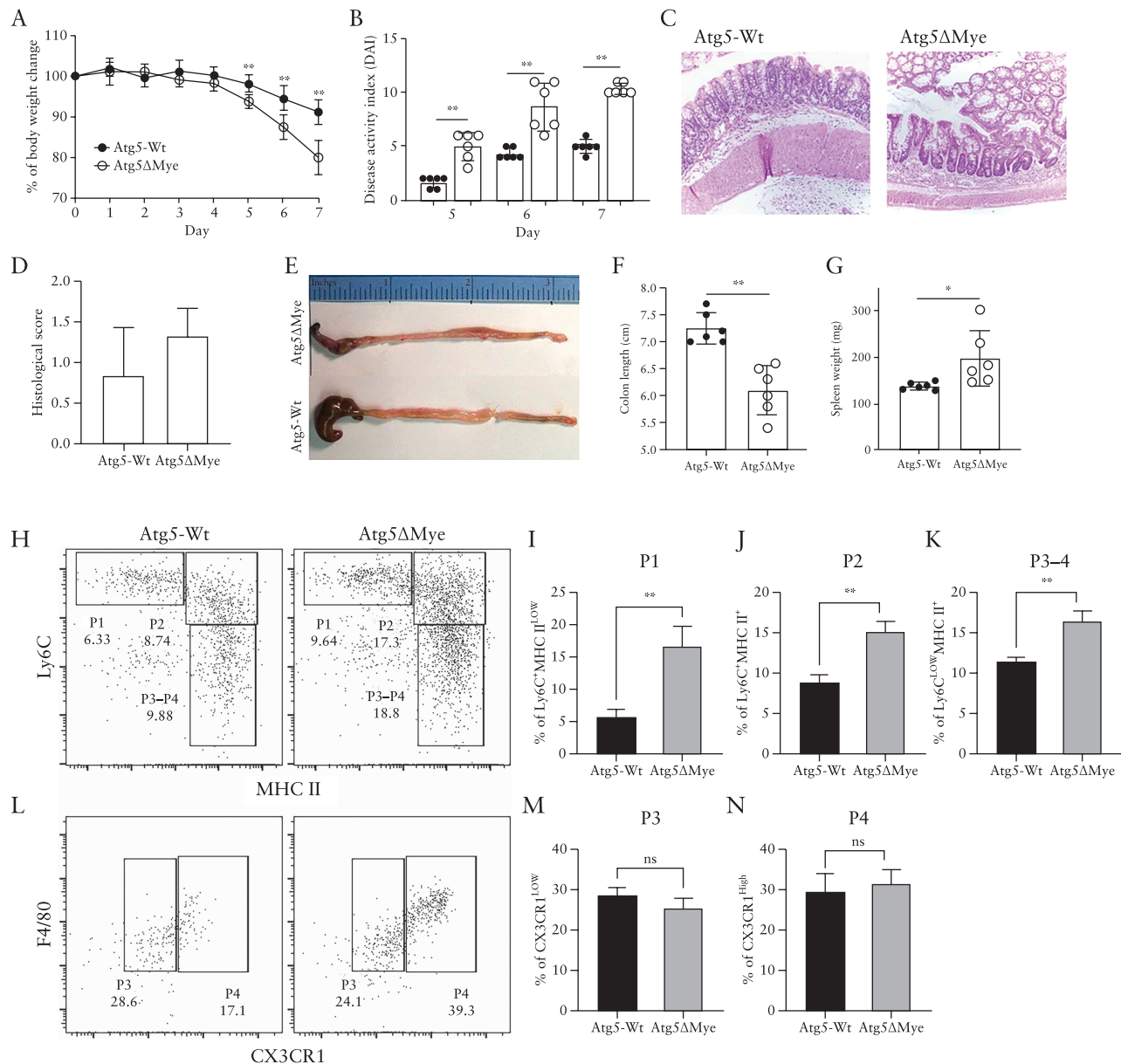


**Figure 2.** Myeloid *Atg5* expression prevents excessive DSS-induced colitis and an accumulation of lamina propria myeloid cells. DSS-induced colitis and myeloid cell response in *Atg5*-Wt and *Atg5*ΔMyc mice. [A] Percent weight loss between *Atg5*-Wt and *Atg5*ΔMyc mice. [B] Disease activity index [DAI] as determined by weight loss, behaviour, acute diarrhoeal response, and mucosal bleeding. [C] H&E staining of colon sections. [D] Histological scores. [E] Representative gross anatomy of the caecum and colon of colitic *Atg5*-Wt and *Atg5*ΔMyc mice. [F] Colon length after colitis. [G] Spleen weight after colitis. [H] Dot plots showing lamina propria [gated on CD45<sup>+</sup>CD11b<sup>+</sup> cells] monocyte waterfall as determined by Ly6C and MHC II staining after colitis. [I] Graph showing percent of P1 [Ly6C<sup>+</sup>MHC II<sup>LOW</sup>] cells. [J] Graph showing percent of P2 [Ly6C<sup>+</sup>MHC II<sup>+</sup>] cells. [K] Graph showing percent of P3-4 [Ly6C<sup>LOW</sup>MHC II<sup>+</sup>] cells. [L] Dot plots showing F4/80 expression and CX3CR1 expression on P3-P4 gated cells in H. [M] Graph showing percent of P3 [Ly6C<sup>LOW</sup>MHC II<sup>+</sup>CX3CR1<sup>LOW</sup>] cells. [N] Graph showing percent of P4 [Ly6C<sup>LOW</sup>MHC II<sup>+</sup>CX3CR1<sup>+</sup>] cells. Representative of three independent experiments, Graphs indicate mean [±SD]; \**p* < 0.05, \*\**p* < 0.01. Two-tailed unpaired Student's *t* tests or by two-way ANOVA with Tukey's post hoc test. DSS, dextran sodium sulphate; H&E, haematoxylin and eosin; SD, standard deviation; ANOVA, analysis of variance.

regulation of the microbiota.<sup>67–70</sup> Autophagy genes appear to be involved in the latter as it was shown the autophagy protein, *Atg16L1*, expressed in myeloid cells from both humans and mice, altered IgA-coated intestinal bacteria at steady state and during inflammation,<sup>26</sup> but it was not confirmed if this increase in IgA-coated bacteria affects the overall microbial community. More recently, another mouse model with a global knockin of the IBD risk allele *ATG16L1 T300A* had an altered gut microbiota preceding colitis induction.<sup>19</sup>

Using *Atg5*ΔMyc mice [myeloid specific loss of autophagy-related 5, *Atg5*, gene], we investigated the importance of *Atg5* expression in myeloid cells in maintaining the intestinal microbiota.<sup>37,56</sup> In comparison with littermate controls [*Atg5*-Wild-type, *Atg5*-Wt], *Atg5*ΔMyc mice showed significant differences in the intestinal microbial composition [Figure 1A]. Similar to what is observed in IBD patients,<sup>59–62,71</sup> *Atg5*ΔMyc mice had a decrease in the phylum Firmicutes [Figure 1B] and an increase in the phylum Bacteroidetes [Figure 1C] compared with *Atg5*-Wt mice. No significant changes

were observed for phyla Actinobacteria and Proteobacteria [Figure 1D and E]. Additionally, the principal coordinate analysis [PCoA] plot and heatmap of bacterial communities revealed tight clustering of Atg5-Wt microbiota that was distinct from Atg5 $\Delta$ Myc microbiota at the genus level [Figure 1F and G], and this was also observed for female mice [Supplementary Figure 1A and B, available as Supplementary data at ECCO-JCC online]. Thus, Atg5 expression in myeloid cells is critical for the maintenance of the intestinal microbiota.

## 2.2. Myeloid Atg5 expression regulates IFN $\gamma$ response in the intestinal microenvironment

The acute DSS-induced colitis model is an innate/wound repair model that is sensitive to the gut microbiota.<sup>72,73</sup> To examine the impact of the microbiota alteration in Atg5 $\Delta$ Myc mice during an inflammatory state, we subjected both Atg5 $\Delta$ Myc and Atg5-Wt mice to DSS-induced acute colitis. Similar to what was reported in mice with an *Atg161l*- or *Atg7*-deficiency specifically in myeloid cells,<sup>26,74</sup> colitis induction in Atg5 $\Delta$ Myc mice resulted in an exacerbated inflammatory response compared with Atg5-Wt mice.

Intestinal epithelial disruption via DSS caused significant weight loss [Figure 2A] as well as acute diarrhoeal response and mucosal bleeding [disease activity index, DAI, Figure 2B] in Atg5 $\Delta$ Myc mice; however, histologically both groups showed inflammation [Figure 2C and D]. Severe inflammation from the caecum to the distal colon of Atg5 $\Delta$ Myc mice was observed [Figure 2E]. The length of the colon was also measured to assess colonic mucosal injury and revealed colonic shortening [Figure 2F]. We also found that the spleen weight of colitic Atg5 $\Delta$ Myc mice was increased [Figure 2G]. Examination of the cellular infiltration in the colonic lamina propria [LP] during DSS-induced colitis revealed a significant increase in polymorphonuclear [PMN] leukocytes [Ly6G<sup>high</sup>CD11b<sup>+</sup>] in colitic Atg5 $\Delta$ Myc mice compared with colitic controls [Supplementary Figure 2A and B, available as Supplementary data at ECCO-JCC online]. We also found an increase in monocytes and macrophages that were distinguished by Ly6C, MHCII, and CX3CR1 expression [Figure 2H–N]. Colonic macrophages are replenished by monocytes through a differentiation process called the monocyte waterfall.<sup>75–78</sup> Ly6C<sup>high</sup>MHCII<sup>-</sup> [P1] monocytes acquire MHCII to become Ly6C<sup>high</sup>MHCII<sup>+</sup> monocytes [P2]. These monocytes then differentiate

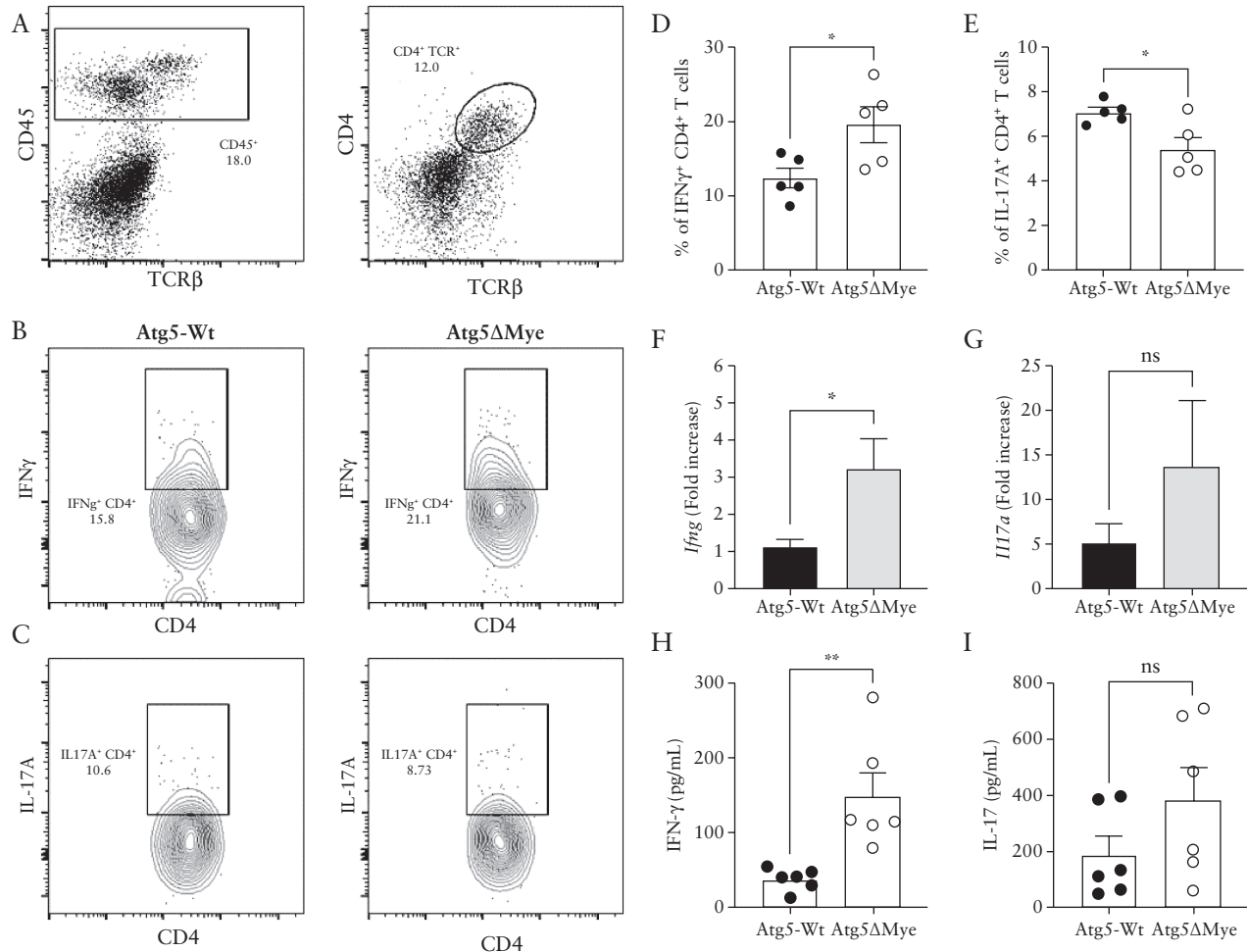


**Figure 3.** Myeloid Atg5 expression prevents excessive IFN $\gamma$ -mediated intestinal inflammation. Analysis of colonic IFN $\gamma$  production after colitis induction. [A] Dot plots showing LP CD4<sup>+</sup> T cells staining after colitis. [B] Intracellular IFN $\gamma$  staining in LP CD4<sup>+</sup> T cells. [C] Intracellular IL-17A staining in LP CD4<sup>+</sup> T cells. [D] Graph showing the percent of IFN $\gamma$ <sup>+</sup>CD4<sup>+</sup> T cells isolated from the LP of colitic mice. [E] Graph showing the percent of IL-17A<sup>+</sup>CD4<sup>+</sup> T cells isolated from the LP of colitic mice. [F] Colonic *Ifng* and [G] *Il17a* gene expression after colitis induction. [H] Colonic IFN $\gamma$  and [I] IL-17 protein expression as determined by ELISA. Representative of three independent experiments. Graphs indicate mean  $\pm$ SD; \* $p$  < 0.05, \*\* $p$  < 0.01, Two-tailed unpaired Student's t tests. LP, lamina propria; ELISA, enzyme-linked immunosorbent assay.

into macrophages Ly6C<sup>+</sup>MHCII<sup>+</sup> [P3-4] after downregulating Ly6C and then become fully mature macrophages by upregulating CX3CR1 [P4]. We find P1 [Figure 2I], P2 [Figure 2J], and the P3-4 mixed [Figure 2K] subsets are significantly increased in the LP of colitic Atg5ΔMyc mice compared with colitic control mice; however, P3 and P4 subsets were not significantly different [Figure 2L–N]. During colitis, pro-inflammatory Ly6C<sup>+</sup>MHCII<sup>+</sup> monocytes [P2] accumulate in the colon,<sup>79</sup> which we find are increased in Atg5ΔMyc mice [Figure 2J]. P4 macrophages from Atg5ΔMyc mice also showed a general increase in TLR4 [Supplementary Figure 2C and G], CD14 [Supplementary Figure 2E and I], and CD115 [Supplementary Figure 2F and J] expression while expressing lower levels of CD206 [Supplementary Figure 2D and H] compared with P4 macrophages isolated from colitic control mice; however, only the levels of CD115 were significantly increased in the LP of colitic Atg5ΔMyc mice. Overall, these results indicate that Atg5 expression in myeloid cells, like Atg7 and Atg16L1, is critical to control acute intestinal inflammation.

The proinflammatory cytokine IL-17 contributes to shaping and regulating the intestinal microbiota. We and others have shown that T cells from mice wherein myeloid cells lack *Atg5* or other autophagy-related genes display skewing towards IL-17 polarisation.<sup>37,39–41</sup> This T cell polarisation is mediated through the dysregulation of cytokines or cellular components that promote IL-17 responses.<sup>43,44</sup> Microbiota differences can also alter T cell polarisation.<sup>80–84</sup> Although the acute DSS model is not solely dependent on B and T cell responses, both participate in the exaggerated presentation of the disease. In fact, T cells have been shown to be the major driver of colonic inflammation in the acute DSS model by Day 4, with a peak at Day 8.<sup>85</sup> Interestingly, we do not see major changes in DAI in Atg5ΔMyc mice until Days 6 and 7 [Figure 2B] when we would expect T cells to be responding. To determine whether an enhanced level of IL-17-producing T cells populating the intestinal mucosa is influencing the microbiota of Atg5ΔMyc mice and contributing to this excess inflammatory response, we isolated and stimulated CD4<sup>+</sup> T cells from the colon lamina propria [LP] of mice during DSS treatment to determine TH polarisation. Interestingly, we observed an increase in IFN $\gamma$ -producing CD4<sup>+</sup> T cells isolated from the colonic LP of Atg5ΔMyc mice [Figure 3A, B, and D]. Colitic colons from Atg5ΔMyc mice also showed an increased IFN $\gamma$  gene and protein expression compared with controls [Figure 3F and H]. Additionally, there was also an increase in IFN $\gamma$ -producing CD4<sup>+</sup> T cells isolated from the mesenteric lymph nodes (mLN) of colitic Atg5ΔMyc mice [Supplementary Figure 3A, available as Supplementary data at ECCO-JCC online]. We also observed a significant reduction in IL-17-producing CD4<sup>+</sup> T cells isolated from the colon of Atg5ΔMyc mice compared with controls [Figure 3A, C, and E]. Although there was a difference in IL-17-producing CD4<sup>+</sup> T cells in the colon, we found no significant difference in IL-17 gene and protein expression in the colon from both colitic Atg5ΔMyc and Atg5-Wt mice [Figure 3G and I] or from mLN CD4<sup>+</sup> T cells [Supplementary Figure 3B].

Our observation that CD4<sup>+</sup> T cells are skewed towards a type 1 immune response in Atg5ΔMyc mice after colitis induction prompted an examination of cytokine expression and TH skewing at steady state. Spontaneous colitis never occurred in Atg5ΔMyc mice but, similar to what was observed during colitis, we observed an increase in IFN $\gamma$ -producing CD4<sup>+</sup> T cells isolated from the colonic LP of Atg5ΔMyc mice [Supplementary Figure 3C and D] with no significant difference in the number of IL-17-producing CD4<sup>+</sup> T cells [Supplementary Figure 3E and F] at steady state. This discrepancy in

IL-17 expression could be tissue-specific, as models in which myeloid cells lack autophagic components and express high levels of IL-17 have been reported for only respiratory infections.<sup>37,40,41</sup> However, others have reported TH1 skewing in ATG16L1T300A knockin mice as well as in conditional myeloid Atg7-deficient mice during intestinal inflammation.<sup>19,26</sup> Furthermore, IFN $\gamma$  has been shown to play an indispensable role in the initiation of acute DSS colitis, and IFN $\gamma$ -deficient mice are protected from acute DSS-induced colitis.<sup>86</sup> Thus, this model is sufficient to show IFN $\gamma$  responses from T cells in Atg5ΔMyc mice. Overall, at steady state and during inflammation, Atg5ΔMyc mice show differences in CD4<sup>+</sup> T cell polarisation in the colon particularly to a type 1 immune response.

### 2.3. Atg5 limits IL-12 production in myeloid cells independent of canonical autophagy

The current paradigm is that an autophagic defect [or loss of an autophagy-related gene] in myeloid cells leads to enhanced IL-1 $\alpha/\beta$  expression.<sup>37–39</sup> The excess production of IL-1 skews lymphocytes to produce IL-17, subsequently promoting IL-17-mediated inflammation. However, we found colitic Atg5ΔMyc mice presented with increased IFN $\gamma$  and no significant difference in IL-17 in the colon microenvironment. This suggests that colonic *Atg5*-deficient myeloid cells are likely to produce other factors that promote TH1 skewing and IFN $\gamma$  production. IL-12p70 [hereafter called IL-12] is a major cytokine involved in TH1 polarisation and is a potent inducer of IFN $\gamma$ .<sup>35,87–89</sup> IL-12 is a heterodimeric protein comprising IL-12p35 and IL-12p40 [IL-12p40 also dimerises with IL-23p19 to form IL-23, a major cytokine maintaining TH17 cells] and is highly expressed by various myeloid cells including macrophages.<sup>35,90–93</sup> We have previously shown that Atg5ΔMyc mice also produce excess IL-12 during tuberculosis infection.<sup>37</sup> Examination of the colon at steady state and during colitis revealed a general increase in IL-12 gene and protein expression [Supplementary Figure 3G–L] in Atg5ΔMyc mice. This increase in colonic IL-12 suggests the cytokines required to promote type 1 immune responses are present in the colonic microenvironment of Atg5ΔMyc mice. Nevertheless, it is unclear if this excess IL-12 is coming from *Atg5*-deficient myeloid cells.

We next set out to determine if *Atg5*-deficient myeloid cells produce excess IL-12. Using bone marrow-derived macrophages [BMM] from Atg5ΔMyc and Atg5-Wt mice, we showed that *Atg5*-deficient macrophages secrete excess IL-12 upon LPS/IFN $\gamma$  stimulation compared with Atg5-Wt macrophages [Figure 4A]. For many cell types, low levels of IL-12p35 are constitutively expressed, whereas IL-12p40 expression occurs primarily in macrophages and dendritic cells, and both increase in response to microbial stimulation.<sup>90–93</sup> We observed no difference in *Il12a* [IL-12p35] and *Il12b* [IL-12p40] gene expression [Supplementary Figure 4A and B, available as Supplementary data at ECCO-JCC online]. Furthermore, there was no difference in cell surface expression of IFN $\gamma$ -receptor, TLR4/MD2, or CD14 between Atg5-Wt and *Atg5*-deficient BMM [Supplementary Figure 4C] that would enable an enhanced response. These data suggest that *Atg5* has a post-transcriptional role in regulating IL-12 secretion.

As mentioned above, *Atg5* assists in autophagosome formation and autophagosome-lysosome fusion. Thus, the genetic deletion of *Atg5* would consequently affect several steps in autophagy. We next considered whether IL-12 was a direct target for autophagic removal. However, endogenous IL-12 and LC3 did not co-localise during stimulation and treatment with bafilomycin A1 [Baf. A1] [Supplementary Figure 4D] in Atg5-Wt or *Atg5*-deficient BMM, suggesting that IL-12

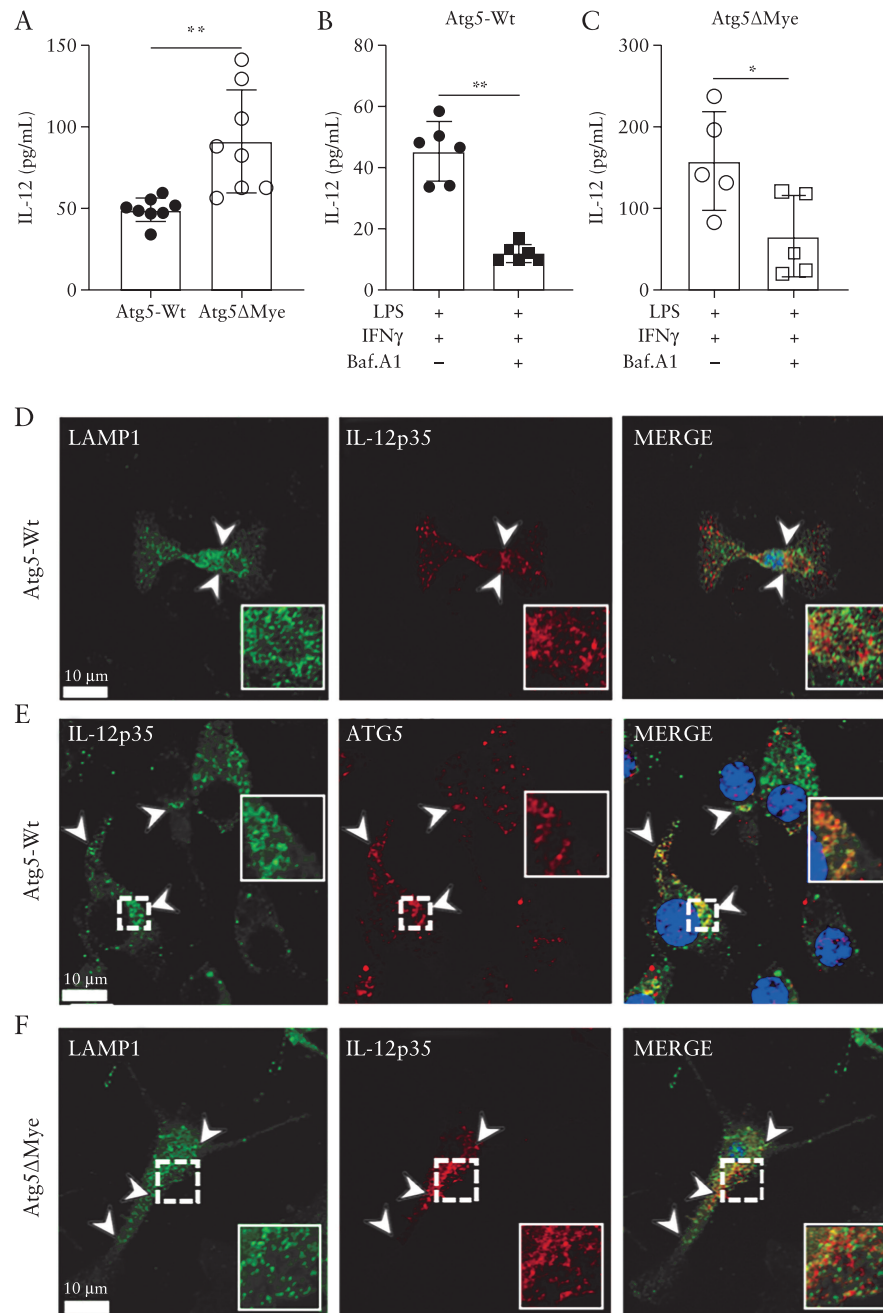


**Figure 4.** Atg5 regulates IL-12 secretion in macrophages. Analysis of IL-12 secretion in macrophages. [A] Detection of IL-12 by ELISA from Atg5-Wt or Atg5ΔMyc BMM after LPS and IFN $\gamma$  stimulation. [B and C] Detection of IL-12 by ELISA from Atg5-Wt [B] or Atg5ΔMyc [C] BMM after LPS and IFN $\gamma$  stimulation in the presence or absence of Baf. A1. Representative of two independent experiments. [D-F] 1–3  $\mu$ m Z-stack images were performed on BMM stimulated with LPS, IFN $\gamma$ , and Baf. A1 using immunofluorescence at 1.6 Zoom by a 63x oil immersion objective. [D] Atg5-Wt BMM were stained for LAMP1 [green] and IL-12p35 [red]. [E] Atg5-Wt BMM were stained for ATG5 [red] and IL-12p35 [green]. [F] Atg5ΔMyc BMM were stained for LAMP1 [green] and IL-12p35 [red]. Representative from 65 images from 15 slides from two independent experiments. Arrows in images indicate puncta co-localising with insets displaying enlargement of indicated region. Scale bars: 10  $\mu$ m. Graphs indicate mean  $\pm$ SD; \* $p$  < 0.05, \*\* $p$  < 0.01, \*\*\* $p$  < 0.001. Two-tailed unpaired Student's t tests. ELISA, enzyme-linked immunosorbent assay; BMM, bone marrow-derived macrophages; LPS, lipopolysaccharide; SD, standard deviation.

is unlikely to be a direct target for autophagic degradation. Baf. A1 is widely used to inhibit autophagic flux by targeting the V-ATPase ATP6V0C/V0 subunit c, but can also de-acidify endosome/lysosome vesicles through the same mechanism.<sup>94,95</sup> Atg5 also regulates acidification and de-acidification of late endosomal compartments<sup>96</sup> and, before stimulation, Atg5-deficient BMM display increased lysotracker staining compared with Atg5-Wt BMM [Supplementary Figure 4E],

suggesting that the loss of Atg5 affects the regulation of vesicles' pH levels.<sup>96,97</sup> Interestingly, Baf. A1 treatment decreased IL-12 secretion in Atg5-Wt BMM [Figure 4B]. Furthermore, treatment of Atg5-deficient BMM with Baf. A1 also reduced IL-12 secretion [Figure 4C]. These data suggest that Atg5 regulates IL-12 secretion through vesicle acidification, and Baf. A1 can compensate for the loss of Atg5 in regulating IL-12 secretion.

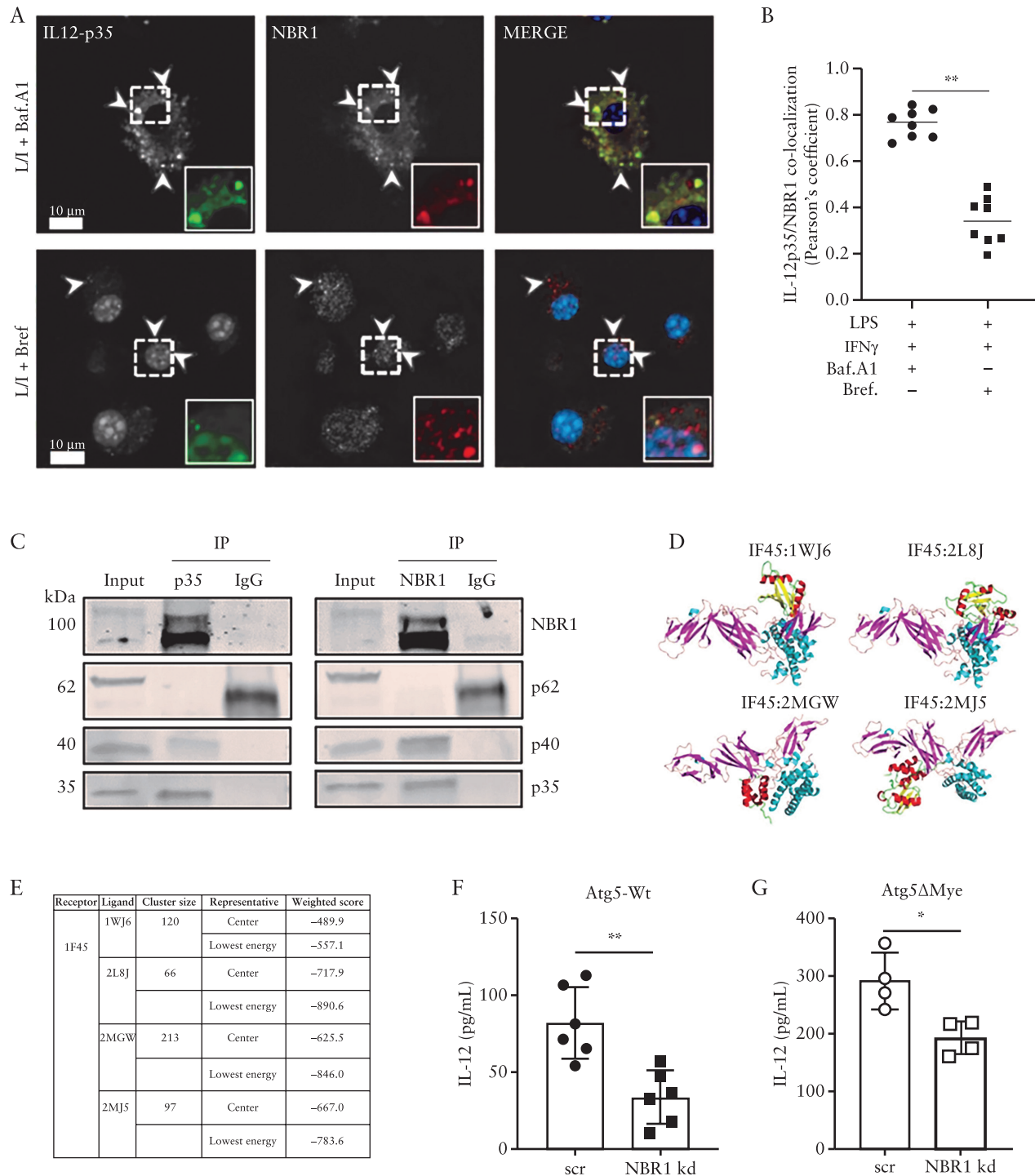


**Figure 5.** NBR1 and IL-12 interaction. Analysis of NBR1 and IL-12 interaction in macrophages. [A] Atg5-Wt BMM were stained for NBR1 [red] and IL-12p35 [green] after LPS and IFN $\gamma$  stimulation and the addition of Bafilomycin A1 [top row] or Brefeldin A [bottom row]. [B] Quantification was performed using Pearson's correlation coefficient [co-localisation] using image analysis. Representative of two independent of experiments and of 10 images from five slides. Arrows in images indicate puncta co-localising with insets displaying enlargement of indicated region. Scale bars: 10  $\mu$ m. [C] Anti-IL-12p35 antibody co-immunoprecipitated NBR1 and IL-12p40, and anti-NBR1 antibody co-immunoprecipitated IL-12p35 and IL-12p40. [D and E] Protein docking between IL12A [PDB ID: 1F45] and NBR1. [D] The docking models and [E] ClusPro docking results for four candidate interaction models between 1F45 and four peptide fragments of NBR1 [PDB IDs: 1WJ6, 2L8J, 2MGW, and 2MJ5]. [F and G] Effects of NBR1 knockdown on IL-12 secretion in Atg5-Wt or Atg5 $\Delta$ Myc BMM. Graphs indicate mean  $\pm$ SD. \*  $p < 0.05$ , \*\*  $p < 0.01$ . Two-tailed unpaired Student's t tests. BMM, bone marrow-derived macrophages; LPS, lipopolysaccharide; SD, standard deviation.

We next examined the intracellular localisation of IL-12 after Baf. A1 treatment. As mentioned above, IL-12 consists of subunits IL-12p35 and IL-12p40. Whereas the IL-12p40 subunit has conventional secretory sequences and can be secreted in its homodimeric

form, the IL-12p35 peptide is leaderless, cannot be secreted as a monomer, and conventional secretion cannot be induced by the addition of a secretory sequence.<sup>90,91,93</sup> The purpose of IL-12p35's constitutive expression remains poorly understood,<sup>90</sup> but a recent report



demonstrated that IL-12p35 is trafficked to late endosomes [LE] before secretion.<sup>98</sup> As observed with total IL-12, Baf. A1 treatment resulted in IL-12p35 accumulation in LE as determined by IL-12p35 [red] and Lamp1 [green] co-localisation [Figure 4D]. White arrows in images indicate puncta co-localising with insets displaying enlargement of indicated region. Interestingly, IL-12p35 [green] co-localised with Atg5 [red] [Figure 4E]. IL-12 [red] co-localisation with Lamp1 [green] was more evident in *Atg5*-deficient BMM [Figure 4F]. Further analysis revealed that IL-12 [red] also co-localised with the LE marker Rab7 [green] [Supplementary Figure 4F], as previously reported.<sup>98</sup> Taken together, our data suggest that Lamp1<sup>+</sup> LEs<sup>99,100</sup> contain IL-12, and the lack of *Atg5* leads to increased levels of IL-12 in these vesicles.

#### 2.4. The sequestosome-1-like receptor NBR1 is involved in IL-12 secretion

Most cytokines are directed by their signal sequence through endoplasmic reticulum [ER]-golgi complex pathway for processing and trafficking, but some inflammatory cytokines, including IL-1 $\beta$  and IL-18, are known to be excreted via alternative strategies.<sup>38,101–105</sup> For IL-1 $\beta$ , the selective autophagy cargo receptor TRIM16 directs IL-1 $\beta$  to LC3-II+ sequestration membranes for secretion.<sup>103</sup> This suggests that other selective cargo receptors, such as the sequestosome-1-like receptors [SLRs: p62/SQSTM1 and NBR1], could act as possible cargo receptors for alternative secretion.<sup>102,105,106</sup> We considered that NBR1 might be responsible for delivering IL-12 to LE for secretion given a homologue of the mammalian NBR1; *Nbr1* from *Schizosaccharomyces pombe* was shown to deliver proteins to LE,<sup>107</sup> and NBR1 accumulates upon autophagy inhibition.<sup>108</sup> Indeed, confocal imaging revealed NBR1 [red] co-localised with IL-12p35 [green] in WT BMM after LPS/IFN- $\gamma$  and Baf. A1 treatment [Figure 5A, top row, and B]; white arrows indicate puncta co-localising. However, this co-localisation was reduced upon brefeldin A [BrefA] treatment, suggesting that NBR1 [red] and IL-12 [green] interaction occurs after IL-12 leaves the ER [Figure 5A, bottom row, and B]. This reduction in co-localisation was not due to enhanced secretion, as IL-12 was undetectable by enzyme-linked immunosorbent assay [ELISA] after LPS/IFN $\gamma$ /brefA treatment [data not shown]. To verify NBR1/IL-12 interaction in macrophages, cell lysates were immunoprecipitated with anti-IL12p35, anti-NBR1, or isotype control antibodies, and subjected to western blot with anti-IL-12p35, anti-IL-12p40, anti-NBR1, and anti-p62 antibodies. Both IL-12p40 and NBR1 co-precipitated with anti-IL-12p35 antibodies [Figure 5C]. Reciprocally, IL-12p35 and IL-12p40 co-precipitated with anti-NBR1 antibodies [Figure 5C]; however, neither probe co-precipitated p62/SQSTM1 [Figure 5C]. This interaction was further verified *in silico* through ClusPro docking,<sup>109</sup> as IL-12 [1F45] interacted with multiple peptide fragments [1WJ6, 2L8J, 2MGW, and 2MJ5] of NBR1 [Figure 5D and E]. Lastly, a knockdown of NBR1 via small interfering RNA [siRNA] in *Atg5*-Wt BMM reduced IL-12 secretion compared with scrambled siRNA control [Figure 5F; Supplementary Figure 4G]. A reduction in IL-12 secretion was also observed in *Atg5*-deficient BMM after NBR1 knockdown, suggesting this interaction is independent of *Atg5* [Figure 5G; Supplementary Figure 4G]. Taken together, our data suggest NBR1 is partially responsible for IL-12 secretion whereby it functions to direct IL-12p35 to LE for secretion.

#### 2.5. IL-12 and the *Atg5 $\Delta$ Myc gut microbiota contribute to the exacerbated intestinal inflammation*

We found the exacerbated intestinal inflammation in *Atg5 $\Delta$ Myc mice coincides with dysregulated IL-12 levels. Although this is the*

first finding linking *Atg5* to IL-12 secretion, IL-12 has been associated with intestinal inflammation<sup>87,110</sup> and it has been targeted therapeutically to attenuate intestinal inflammation. In both chemically induced colitis and genetic-deficient mouse models of colitis, antibodies against IL-12 prevented intestinal inflammation.<sup>110–114</sup> Clinical trials have also been performed in individuals with IBD, using antibodies against the IL-12p40 subunit.<sup>48,115–119</sup> These antibodies target both IL-12 and IL-23 pathways and has proven to be a safe and effective treatment approach in patients with IBD. Antibodies against IL-12/IL-23 also show efficacy in patients who failed treatment with anti-TNF- $\alpha$  agents, and the efficacy is more pronounced among secondary non-responders. Nevertheless, it unclear if IL-12 is leading to the changes in the gut microbiota and susceptibility to DSS-induced colitis we observe in *Atg5 $\Delta$ Myc mice. Given the antibodies target both IL-12 and IL-23, we decided to target only IL-12 by crossing *Atg5 $\Delta$ Myc mice with IL-12p35-deficient mice<sup>120</sup> to generate *Atg5 $\Delta$ Myc-IL12KO mice. We first examined the colonic microbiota at steady state in all three groups of mice [i.e., *Atg5*-Wt, *Atg5 $\Delta$ Myc and *Atg5 $\Delta$ Myc-IL12KO]. *Atg5 $\Delta$ Myc-IL12KO mice showed a global change in the intestinal microbial composition in comparison with *Atg5 $\Delta$ Myc mice, particularly an increase in the phylum Firmicutes [Supplementary Figure 5A, available as Supplementary data at ECCO-JCC online]. Furthermore, the PCoA plots and heatmap show clustering of the bacterial communities [at genus level] of the *Atg5 $\Delta$ Myc-IL12KO and *Atg5*-Wt colonic mice which was separated from the bacterial community in the *Atg5 $\Delta$ Myc mice [Figure 6A and B].*********

We next examined *Atg5 $\Delta$ Myc-IL12KO mice response to DSS-induced colitis. *Atg5 $\Delta$ Myc-IL12KO mice were protected from DSS-induced colitis compared with *Atg5 $\Delta$ Myc mice. *Atg5 $\Delta$ Myc-IL12KO mice suffered minimal weight loss, showed no shortening of the colon after colitis induction, and had reduced spleen weights [Figure 6C–E]; however, no major changes were observed by histology [Supplementary Figure 5B and C]. There was also a decrease in *Ifng* gene expression in the colon after colitis induction in *Atg5 $\Delta$ Myc-IL12KO mice, but no change in *Il17a* gene expression between both groups of mice [Figure 3F and G]. Isolation and stimulation of colonic LP CD4<sup>+</sup> T cells showed a decrease in IFN $\gamma$ -producing CD4<sup>+</sup> T cells from *Atg5 $\Delta$ Myc-IL12KO mice compared with *Atg5 $\Delta$ Myc mice [Figure 6H and I]. Additionally, we observed a decrease in the percent of IFN $\gamma$ -producing CD4<sup>+</sup> T cells from the mLN of *Atg5 $\Delta$ Myc-IL12KO mice compared with *Atg5 $\Delta$ Myc mice [Supplementary Figure 5D]. However, *Atg5 $\Delta$ Myc-IL12KO mLN CD4<sup>+</sup> T cells did produce more IL-17 [Supplementary Figure 5E]. This change in IL-17 expression is likely due to *Atg5*-deficient myeloid cells producing excess IL-1.<sup>37</sup> Nevertheless, genetic deletion of IL-12p35 from mice in which myeloid cells also lack *Atg5* restores the microbiota and protects against DSS-induced colitis.**********

The DSS-induced colitis model is sensitive to the gut microbiota.<sup>72,73</sup> The restoration of the microbiota in *Atg5 $\Delta$ Myc-IL12KO mice [Figure 6A and B] which coincides with attenuated intestinal inflammation suggest that the *Atg5 $\Delta$ Myc-associated gut microbiota may play a role in the exacerbated inflammation observed in *Atg5 $\Delta$ Myc mice. Therefore, we performed a faecal microbiota transplant [FMT] in *Atg5 $\Delta$ Myc mice to examine the pathogenic potential of the *Atg5 $\Delta$ Myc-associated gut microbiota. First, the microbiota was ablated in a several groups of *Atg5 $\Delta$ Myc mice via antibiotic treatment and microbiota was collected from fresh stool samples from either *Atg5 $\Delta$ Myc or *Atg5*-Wt mice. Antibiotic-treated *Atg5 $\Delta$ Myc mice were then orally gavaged with *Atg5*-Wt-associated microbiota, *Atg5 $\Delta$ Myc-associated microbiota, or carrier solution. One week after FMT, mice were subjected to DSS-supplemented*********

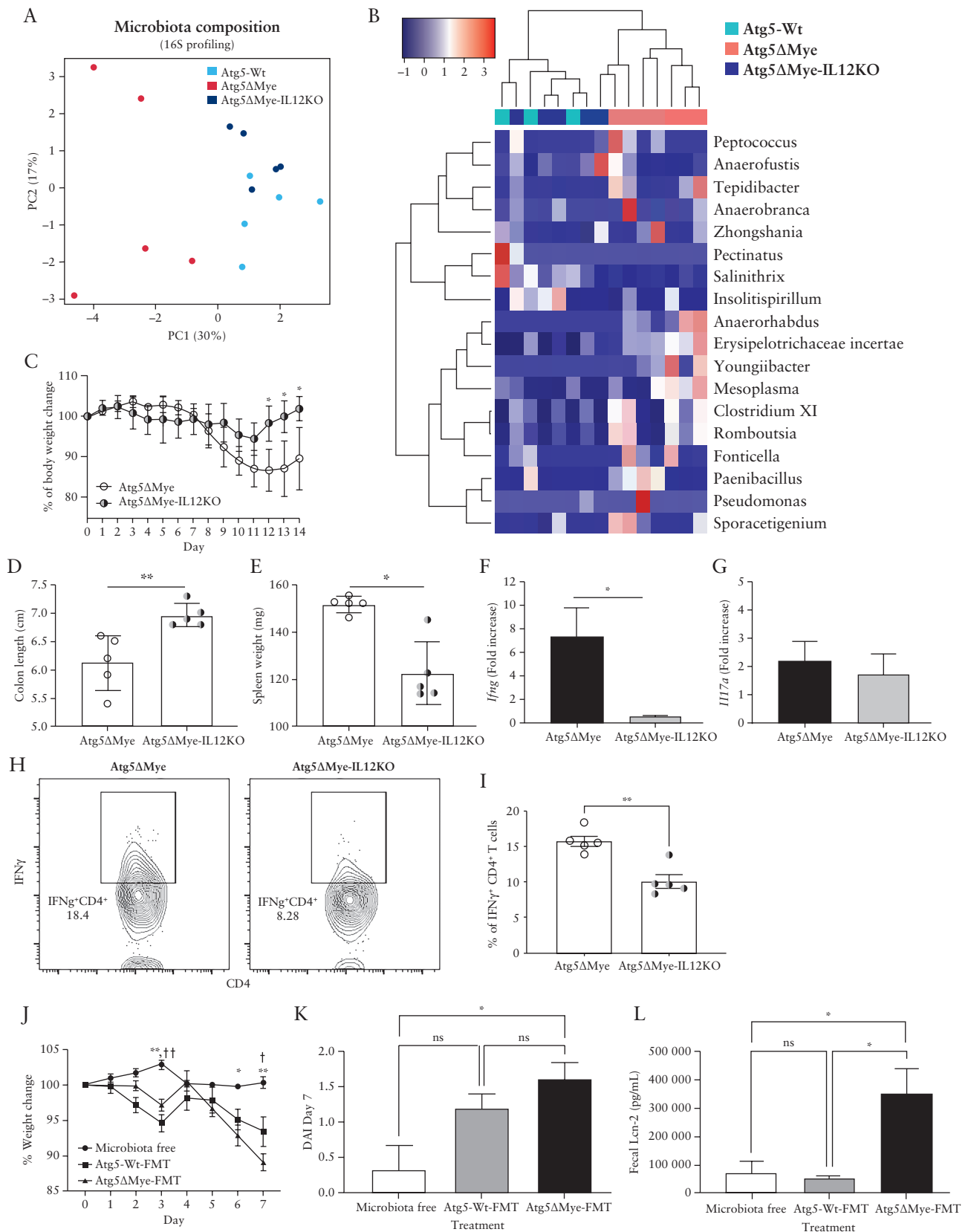


**Figure 6.** Limiting IL-12 in mice with a selective *Atg5*-deficiency in myeloid cells restores the intestinal microbiota and alleviates inflammation. Bacterial composition as assessed by 16S rRNA sequencing from freshly collected stool of *Atg5* $\Delta$ Mye and *Atg5* $\Delta$ Mye-IL12KO mice before colitis induction [ $n = 5$  per group]. [A] Principal coordinates analysis [PCoA] plot of microbiota composition [genus level]. [B] Heatmap of the relative abundance of colonic microbes [genus level]. A  $t$  test was used to measure specific microbiome species abundance between groups. Adjusted  $p$ -value  $>0.05$  was used as significant threshold.

water for 7 days. Daily assessment revealed significant weight loss in Atg5ΔMyc mice receiving Atg5ΔMyc microbiota compared with microbiota-free Atg5ΔMyc mice [Figure 6J]. This was also observed in Atg5ΔMyc mice receiving Atg5-Wt microbiota when compared with microbiota-free Atg5ΔMyc mice [Figure 6J]. Interestingly, microbiota-free Atg5ΔMyc mice subjected to DSS had minimal weight loss. Furthermore, the DAI revealed a significant difference between Atg5ΔMyc mice receiving FMT of Atg5ΔMyc microbiota compared with microbiota-free Atg5ΔMyc mice at Day 7 [Figure 6J; Supplementary Figure 5F]. Assessment of the stool for lipocalin-2 [Lcn-2], a marker of intestinal inflammation,<sup>121–123</sup> at Day 7 revealed FMT of Atg5ΔMyc microbiota had significantly increased faecal Lcn-2 levels compared with Atg5ΔMyc mice with no FMT as well as mice receiving a FMT of Atg5-Wt microbiota [Figure 6K]. Additionally, proximal colons were immediately removed, cleaned, and then incubated for 4 h in RPMI.<sup>124</sup> After the incubation period, the colon and supernatant [concentrated through centrifugation] were prepared for IL-12p35 immunoblot [Supplementary Figure 5G–I]. No significant change was observed for the colon between FMT-treated mice, but the concentrated supernatant from the colon of Atg5ΔMyc mice receiving FMT of Atg5ΔMyc microbiota showed an increase in IL-12 [Supplementary Figure 5G and I]. Overall, this suggests that the gut microbiota of Atg5ΔMyc mice also contributes to the increased IL-12 and exacerbated colitis we have observed [Figure 2].

### 3. Discussion

This work identifies a role for Atg5 in myeloid cells in unconventional cytokine secretion that consequently affects intestinal homeostasis. Additionally, it adds to the plethora of functions described for Atg5.<sup>96,97,125–129</sup> Along with these studies, this work establishes a new non-autophagy, immunological role for Atg5 in promoting TH1 responses. In the context of IBD and autophagy-related proteins [Atg], GWAS have only identified *ATG16L1* variants.<sup>3</sup> Nevertheless, animal models with an Atg5-deficiency display a similar phenotype to Atg16L1-deficient mice.<sup>14</sup> Interestingly, the levels of *ATG5* and the function of autophagy [and possibly other *ATG5* functions] are decreased in IBD patient samples. This decrease in *ATG5* expression and autophagy activity in IBD patients is linked to an increased expression of the microRNA miR30C that acts to downregulate *ATG5* expression.<sup>55,130</sup> Therefore, inhibiting Atg5 expression and function, described here in only myeloid cells, ultimately alters the intestinal microenvironment.

As previously reported, Atg5-deficient myeloid cells produce excess pro-inflammatory cytokines including IL-1α and IL-1β.<sup>37,38</sup> Thus, we cannot dismiss that either cytokine contributes to the excess IFNγ observed in Atg5cKO mice, as IL-1 can synergise with IL-12 to enhance IFNγ production and TH1 skewing.<sup>131,132</sup> Although we and others did not find any changes in colonic IL-17-producing cells in mice with a genetic deletion of Atg5 or Atg7 in myeloid cells,<sup>37,74</sup> both colonic TH17 and TH1 cells were found to be increased in

*ATG16L1* T300A knockin mice.<sup>19</sup> Given that Atg5ΔMyc-IL12KO mice were protected against colitis induction, these results together suggest that IL-12 is a key cytokine driving intestinal pathology and TH1 skewing in our model.

This similarity in intestinal TH1 responses between these mouse models is likely linked to the functional role of Atg5, Atg7, and Atg16L1. All three proteins are involved in some aspect of the autophagy process as well as endosome and lysosome regulation.<sup>12,107,133</sup> The role of the TH17 response in driving intestinal pathology is up for debate as there is strong evidence suggesting that IL-17 may have a protective role in the intestine. Exacerbated intestinal inflammation was reported in *Il17a*-deficient mice or after *in vivo* blockade of IL-17 during DSS-induced colitis.<sup>47,49</sup> Furthermore, in clinical trials for IBD patients, targeting IL-17 or IL-17R worsened symptoms, leading to early clinical trial termination.<sup>46,134</sup> Nevertheless, this does not rule out the effects of increased levels of IL-17 during intestinal inflammation.<sup>30,35,45</sup>

Alterations in the gut microbiota have also been observed in *ATG16L1* T300A knockin mice. Similar to our findings, *ATG16L1* T300A knockin mice also had a decrease in the phylum Firmicutes and an increase in the phylum Bacteroidetes.<sup>19</sup> It is unclear if these microbiota changes in *ATG16L1* T300A knockin mice are due specifically to myeloid cells, since all cells including the intestinal epithelium express the *ATG16L1* T300A gene in this mouse model. Furthermore, it is unclear if a certain genus that is lost/decreased [Firmicutes] or gained/increased [Bacteroidetes] is the driver of intestinal inflammation in Atg5Myc mice. A caveat of our FMT study is the potential loss of strictly anaerobic microorganisms after stool collection and processing. Nevertheless, the identification of the microorganism[s] driving intestinal inflammation could prove beneficial in individuals who have IBD associated with an autophagy risk loci<sup>134</sup>; however, this is out of the scope of this study. Additionally, IL-17 also plays a major role in regulating mucosal IgA production.<sup>136,137</sup> Interestingly, increased IgA-coated bacteria were found in mice that lack Atg16L1 in myeloid cells, as well as in the stool of Crohn's disease patients who were homozygous for the *ATG16L1* T300A risk allele.<sup>26</sup> Additionally, deletions or polymorphisms of autophagy genes in myeloid cells alter bacterial clearance, suggesting that there are multiple mechanisms by which autophagy genes regulate host-microbiota interactions. Our data suggest that myeloid cells likely have a strong contribution in maintaining the microbiota through Atg5's action on IL-12 secretion.

The autophagic process and the genes that regulate autophagy are crucial for intestinal homeostasis. Autophagy is required for the maintenance of tight junction integrity, gut-commensal homeostasis, and control of invasive bacteria at the intestinal epithelium.<sup>13–18,20–22,74,138</sup> Multiple lines of evidence also suggest that autophagy regulates inflammatory cytokines.<sup>37,38,139–141</sup> These attributes make modulation of autophagy or single autophagic proteins an excellent therapeutic target. Nevertheless, it is critical to understand the function of these individual proteins, given they can modulate different TH responses. In fact, reagents that are known

[C] Percent weight loss between Atg5ΔMyc and Atg5ΔMyc-IL12KO mice. [D] Colon length after colitis. [E] Spleen weight after colitis. [F] Colonic *Irfng* and [G] *Il17a* gene expression after colitis induction. [H] Intracellular IFNγ staining in LP CD4<sup>+</sup>T cells after colitis induction. [I] Graph showing the percent of IFNγ<sup>+</sup>CD4<sup>+</sup>T cells isolated from the LP of colitic mice. [J] Percent weight loss between Atg5ΔMyc mice receiving [●] no microbiota, FMT of [■] Atg5-Wt microbiota, or [▲] Atg5ΔMyc microbiota [Atg5-WT FMT vs no FMT, \*Atg5ΔMyc FMT vs no FMT]. [K] Disease activity index [DAI] as determined by weight loss, behaviour, acute diarrhoeal response and mucosal bleeding at Day 7. [L] Faecal Lcn-2 levels as detected by ELISA from FMT Atg5ΔMyc groups. Representative of two-three independent experiments. Graphs indicate mean [±SD]. \* or †p < 0.05, \*\* or ††p < 0.01. Two-tailed unpaired Student's t tests or by one- or two-way ANOVA with Tukey's post hoc test. LPS, lipopolysaccharide; SD, standard deviation; LP, lamina propria; ELISA, enzyme-linked immunosorbent assay; FMT, faecal microbiota transplant; ANOVA, analysis of variance.

to target autophagy activation, such as rapamycin, increase IL-12 secretion.<sup>142,143</sup> Additionally chloroquine, a known inhibitor of autophagosome-lysosome fusion, reduces IL-12 secretion<sup>144</sup> likely through a similar mechanism as does Baf. A1. These reagents have been used with some clinical efficacy in IBD patients and animal models of IBD.<sup>145–148</sup> It is unclear if these effects were due to IL-12 regulation, but targeting IL-12, specifically the IL-12p40 subunit that is shared with IL-23, has also proven beneficial for some IBD patients.<sup>35,48,149</sup> Therefore, understanding how autophagy or single autophagic proteins regulate pro-inflammatory cytokines will allow precision in modulating the immune system in chronic inflammatory conditions like IBD. Last, targeting these autophagy proteins or their functions could be an alternative in mitigating problems associated with biologics, including loss of function, immunogenicity, and cost.<sup>150</sup>

In conclusion, our data support a novel role for Atg5 expression in myeloid cells in regulating intestinal homeostasis. Atg5 expression in myeloid cells controls the IL-12-IFN $\gamma$  pathway that influences the microbiota and limits this pathway during colitis [Supplementary Figure 5J]. Mechanistically, we show that both Atg5 and the cargo receptor NBR1 regulate IL-12 secretion in myeloid cells. Specifically, we propose that NBR1 shuttles IL-12 to LE, whereby Atg5 functions to control the pH of these IL-12-containing vesicles for secretion. A genetic deletion of Atg5 results in dysregulation of IL-12 secretion as well as the accumulation of SLRs such as NBR1,<sup>108</sup> which could potentially allow for increased accumulation of IL-12 in LE. Consequently, these attributes increase IL-12 secretion. A reduction in IL-12 secretion could be achieved by removing NBR1 or reducing LE/lysosomal pH with Baf. A1, even in the absence of Atg5 expression. Nevertheless, the dysregulation of IL-12 in Atg5 $\Delta$ Mye mice leads to alterations of the microbiota and severe colitis when the intestinal barrier is disrupted.

## 4. Materials and Methods

### 4.1. Animals

The transgenic Atg5 $\Delta$ Mye mice [myeloid specific Atg5 deletion] and Atg5-Wt mice have previously been characterised.<sup>56</sup> B6.129S1-*Il12a*<sup>tm1imj</sup>/J [IL-12p35-deficient mice] were purchased from JAX [002692]<sup>119</sup> and crossed to Atg5 $\Delta$ Mye mice to generate Atg5 $\Delta$ Mye-IL12KO mice. All mice were genotyped for the presence of *Atg5*, *Il12a* or Cre expression by Transnetyx Inc. All experiments were approved by the Institutional Animal Care and Use Committee of the University of New Mexico Health Sciences Center, in accordance with the National Institutes of Health guidelines for use of live animals. The University of New Mexico Health Sciences Center is accredited by the American Association for Accreditation of Laboratory Animal Care.

### 4.2. Intestinal inflammation model

For dextran sodium sulphate [DSS]-induced colitis, mice were provided 2.5% DSS [colitis grade, ~30 000–50 000 MW; MP Biomedicals] in drinking water ad libitum. Reagents used for *in vivo* treatment as well as sample collection and stimulation are included in Table S1, available as Supplementary data at ECCO-JCC online.

### 4.3. Microbiota analysis

Fresh faecal samples from Atg5-Wt, Atg5 $\Delta$ Mye, and Atg5 $\Delta$ Mye-IL-12KO mice were collected fresh in sterile tubes and flash-frozen. Microbial communities were determined by sequencing of the 16S

rRNA as previously reported,<sup>151</sup> with minor modifications described below. Microbial DNA was isolated from faeces using the ZymoBIOMICS DNA Miniprep Kit [Zymo Research] following manufacturer's recommendations. Variable regions V-3 through V-4 of the 16S rRNA gene were amplified by polymerase chain reaction [PCR] using 100 ng input of DNA for each sample in duplicate, using primers 319F- [5'-ACTCCTRCGGGAGGCAGCAG-3'] and 806R- [5'-GACAGGACTACHVGGGTATCTAATCC-3'] containing Nextera adapter overhangs. A second PCR was performed with Nextera $\text{\textcircled{R}}$  XT Index Kit v2 Set A [Illumina] to complete the adapter and add unique sample-specific barcodes. After each PCR, a clean-up with AxyPrep Fragment Select-I magnetic beads [Axygen Biosciences] was completed, and all PCR reactions were run on an Applied Biosystems 2720 Thermal Cycler. Indexed samples were combined to yield duplicate 300 ng pools, followed by the creation and denaturation of a 4-nM library, and paired 250-bp sequencing runs were completed on the Illumina MiSeq using v3 sequencing chemistry [Illumina]. All reagents and kits are listed in Table S2, available as Supplementary data at ECCO-JCC online.

### 4.4. Microscopy and image analysis

For confocal microscopy, macrophages were plated at 100 k cells per well on 18-mm glass coverslips and stimulated with LPS [500 ng/mL] and IFN $\gamma$  [10 ng/mL] for 8 h and treated with BrefA [10 nM] or Baf. A1 [10 nM] for 2 h. Cells were then fixed with 4% PFA followed by a wash with 1x PBS. Blocking buffer contained PBS with 50% FBS, 2% BSA, and 0.1% saponin. After a 1-h stain in primary antibody, cells were washed with PBS then followed by 1-h stain in blocking buffer containing secondary antibody. Cells were mounted using ProLong Gold Antifade with DAPI and imaged using the Zeiss LSM 800 Airyscan Confocal microscope with a 63x oil objective lens. Images were processed using Zen Software and Adobe Photoshop [version CC 2019]. All primary and secondary antibodies used for confocal staining are listed in Table S3, available as Supplementary data at ECCO-JCC online.

### 4.5. Statistical analysis

Statistical analysis was performed as described in figure legends, and graphs generated display mean ( $\pm$  standard deviation [SD]) and were obtained using Prism software. Microbiome data were sequenced and processed by Illumina's service laboratory using their in-house analysis pipeline. Cluster analysis was performed using heatmap3<sup>152</sup> package in R. T testing was used to measure specific microbiome species abundance between conditions. Adjusted *p*-value >0.05 was used as significant threshold. Principal coordinate analysis was conducted in R. Confocal images statistical analysis and additional software Pearson's correlation coefficient were acquired from BMM images using Huygens's Deconvolution Scientific Volume Image Software [UNM Fluorescence Microscopy and Cell Imaging shared resource]. Quantification figures were also made using Prism, and confocal image figures were constructed using Adobe Illustrator [version CC 2019]. All other data were analysed using one-way analysis of variance [ANOVA] or two-tailed unpaired Student's *t* test [Prism].

## Funding

Supported in part by the National Center for Research Resources and the National Center for Advancing Translational Sciences of the National Institutes of Health [NIH] through grant no. UL1TR001449 [EFC], KL2TR001448 [EFC] and in part by NIH grant P20GM121176 [EFC], and the Bioinformatics Shared Resource at University of New Mexico Comprehensive Cancer Center

with grant P30CA118100 [YG]. SMG was supported in part by the Infectious Disease and Inflammation Program pre-doctoral T32 training grant, National Institutes of Health/National Institute of Allergy and Infectious Diseases grant T32AI007538.

## Conflict of Interest

The authors declare no conflict of interest.

## Author Contributions

SDM and SMG performed all analysis with the help from YG, ZERW, JRB, RRG, AJH, JGI, and SBB. SDM, ZERW, YG, KCS, and DLD contributed to microbiota sequencing and analysis. SMG, JRB, and SBB participated in imaging and analysis. JGI, SBB, and VD provided reagents and animals. SDM and SMG participated in writing the manuscript. EFC designed the study, analysed data and wrote the paper. All authors approved the final version of the manuscript.

## Supplementary Data

Supplementary data are available at *ECCO-JCC* online.

## References

- Schirmer M, Garner A, Vlamakis H, Xavier RJ. Microbial genes and pathways in inflammatory bowel disease. *Nat Rev Microbiol* 2019;17:497–511.
- Brest P, Lapaquette P, Souidi M, et al. A synonymous variant in IRGM alters a binding site for miR-196 and causes deregulation of IRGM-dependent xenophagy in Crohn's disease. *Nat Genet* 2011;43:242–5.
- Hampe J, Franke A, Rosenstiel P, et al. A genome-wide association scan of nonsynonymous SNPs identifies a susceptibility variant for Crohn disease in ATG16L1. *Nat Genet* 2007;39:207–11.
- Henckaerts L, Cleynen I, Brinar M, et al. Genetic variation in the autophagy gene ULK1 and risk of Crohn's disease. *Inflamm Bowel Dis* 2011;17:1392–7.
- Lahiri A, Hedl M, Abraham C. MTMR3 risk allele enhances innate receptor-induced signaling and cytokines by decreasing autophagy and increasing caspase-1 activation. *Proc Natl Acad Sci U S A* 2015;112:10461–6.
- Lassen KG, Xavier RJ. Mechanisms and function of autophagy in intestinal disease. *Autophagy* 2018;14:216–20.
- Levine B, Kroemer G. Biological functions of autophagy genes: a disease perspective. *Cell* 2019;176:11–42.
- McCarroll SA, Huett A, Kuballa P, et al. Deletion polymorphism upstream of IRGM associated with altered IRGM expression and Crohn's disease. *Nat Genet* 2008;40:1107–12.
- Rioux JD, Xavier RJ, Taylor KD, et al. Genome-wide association study identifies new susceptibility loci for Crohn disease and implicates autophagy in disease pathogenesis. *Nat Genet* 2007;39:596–604.
- Roberts RL, Gearry RB, Hollis-Moffatt JE, et al. IL23R R381Q and ATG16L1 T300A are strongly associated with Crohn's disease in a study of New Zealand Caucasians with inflammatory bowel disease. *Am J Gastroenterol* 2007;102:2754–61.
- Yamazaki K, Onouchi Y, Takazoe M, Kubo M, Nakamura Y, Hata A. Association analysis of genetic variants in IL23R, ATG16L1 and 5p13.1 loci with Crohn's disease in Japanese patients. *J Hum Genet* 2007;52:575–83.
- Galluzzi L, Baehrecke EH, Ballabio A, et al. Molecular definitions of autophagy and related processes. *EMBO J* 2017;36:1811–36.
- Cadwell K, Liu JY, Brown SL, et al. A key role for autophagy and the autophagy gene Atg16l1 in mouse and human intestinal Paneth cells. *Nature* 2008;456:259–63.
- Cadwell K, Patel KK, Komatsu M, Virgin HW 4th, Stappenbeck TS. A common role for Atg16L1, Atg5 and Atg7 in small intestinal Paneth cells and Crohn disease. *Autophagy* 2009;5:250–2.
- Matsuzawa-Ishimoto Y, Shono Y, Gomez LE, et al. Autophagy protein ATG16L1 prevents necroptosis in the intestinal epithelium. *J Exp Med* 2017;214:3687–705.
- Night PK, Hu CA, Ma TY. Autophagy enhances intestinal epithelial tight junction barrier function by targeting claudin-2 protein degradation. *J Biol Chem* 2015;290:7234–46.
- Patel KK, Miyoshi H, Beatty WL, et al. Autophagy proteins control goblet cell function by potentiating reactive oxygen species production. *EMBO J* 2013;32:3130–44.
- Wong M, Ganapathy AS, Suchanec E, Laidler L, Ma T, Nighot P. Intestinal epithelial tight junction barrier regulation by autophagy-related protein ATG6/beclin 1. *Am J Physiol Cell Physiol* 2019;316:C753–65.
- Lavoie S, Conway KL, Lassen KG, et al. The Crohn's disease polymorphism, ATG16L1 T300A, alters the gut microbiota and enhances the local Th1/Th17 response. *Elife* 2019;8:e39982.
- Bel S, Pendse M, Wang Y, et al. Paneth cells secrete lysozyme via secretory autophagy during bacterial infection of the intestine. *Science* 2017;357:1047–52.
- Benjamin JL, Sumpter R Jr, Levine B, Hooper LV. Intestinal epithelial autophagy is essential for host defense against invasive bacteria. *Cell Host Microbe* 2013;13:723–34.
- Burger E, Araujo A, López-Yglesias A, et al. Loss of paneth cell autophagy causes acute susceptibility to *Toxoplasma gondii*-mediated inflammation. *Cell Host Microbe* 2018;23:177–90.e4.
- Chauhan S, Mandell MA, Deretic V. IRGM governs the core autophagy machinery to conduct antimicrobial defense. *Mol Cell* 2015;58:507–21.
- Homer CR, Richmond AL, Rebert NA, Achkar JP, McDonald C. ATG16L1 and NOD2 interact in an autophagy-dependent antibacterial pathway implicated in Crohn's disease pathogenesis. *Gastroenterology* 2010;139:1630–41.
- Singh SB, Davis AS, Taylor GA, Deretic V. Human IRGM induces autophagy to eliminate intracellular mycobacteria. *Science* 2006;313:1438–41.
- Zhang H, Zheng L, McGovern DP, et al. Myeloid ATG16L1 facilitates host-bacteria interactions in maintaining intestinal homeostasis. *J Immunol* 2017;198:2133–46.
- Angelidou I, Chrysanthopoulou A, Mitsios A, et al. REDD1/autophagy pathway is associated with neutrophil-driven IL-1 $\beta$  inflammatory response in active ulcerative colitis. *J Immunol* 2018;200:3950–61.
- Coccia M, Harrison OJ, Schiering C, et al. IL-1 $\beta$  mediates chronic intestinal inflammation by promoting the accumulation of IL-17A secreting innate lymphoid cells and CD4<sup>+</sup> Th17 cells. *J Exp Med* 2012;209:1595–609.
- Dragasevic S, Stankovic B, Sokic-Milutinovic A, et al. Importance of TLR9-IL23-IL17 axis in inflammatory bowel disease development: gene expression profiling study. *Clin Immunol* 2018;197:86–95.
- Jiang W, Su J, Zhang X, et al. Elevated levels of Th17 cells and Th17-related cytokines are associated with disease activity in patients with inflammatory bowel disease. *Inflamm Res* 2014;63:943–50.
- Kanai T, Mikami Y, Sujino T, Hisamatsu T, Hibi T. ROR $\gamma$ t-dependent IL-17A-producing cells in the pathogenesis of intestinal inflammation. *Mucosal Immunol* 2012;5:240–7.
- Liu Z, Yadav PK, Xu X, et al. The increased expression of IL-23 in inflammatory bowel disease promotes intraepithelial and lamina propria lymphocyte inflammatory responses and cytotoxicity. *J Leukoc Biol* 2011;89:597–606.
- Mao L, Kitani A, Strober W, Fuss IJ. The role of NLRP3 and IL-1 $\beta$  in the pathogenesis of inflammatory bowel disease. *Front Immunol* 2018;9:2566.
- Menghini P, Corridoni D, Butto LF, et al. Neutralization of IL-1 $\alpha$  ameliorates Crohn's disease-like ileitis by functional alterations of the gut microbiome. *Proc Natl Acad Sci U S A* 2019;116:26717–26.
- Moschen AR, Tilg H, Raine T. IL-12, IL-23 and IL-17 in IBD: immunobiology and therapeutic targeting. *Nat Rev Gastroenterol Hepatol* 2019;16:185–96.
- Shouval DS, Biswas A, Kang YH, et al. Interleukin 1 $\beta$  mediates intestinal inflammation in mice and patients with interleukin 10 receptor deficiency. *Gastroenterology* 2016;151:1100–4.
- Castillo EF, Dekonenko A, Arko-Mensah J, et al. Autophagy protects against active tuberculosis by suppressing bacterial burden and inflammation. *Proc Natl Acad Sci U S A* 2012;109:E3168–76.

38. Dupont N, Jiang S, Pilli M, Ornatowski W, Bhattacharya D, Deretic V. Autophagy-based unconventional secretory pathway for extracellular delivery of IL-1 $\beta$ . *EMBO J* 2011;30:4701–11.
39. Peral de Castro C, Jones SA, Ni Cheallaigh C, et al. Autophagy regulates IL-23 secretion and innate T cell responses through effects on IL-1 secretion. *J Immunol* 2012;189:4144–53.
40. Reed M, Morris SH, Owczarczyk AB, Lukacs NW. Deficiency of autophagy protein Map1-LC3b mediates IL-17-dependent lung pathology during respiratory viral infection via ER stress-associated IL-1. *Mucosal Immunol* 2015;8:1118–30.
41. Watson RO, Manzanillo PS, Cox JS. Extracellular M. tuberculosis DNA targets bacteria for autophagy by activating the host DNA-sensing pathway. *Cell* 2012;150:803–15.
42. Zhang M, Kenny SJ, Ge L, Xu K, Schekman R. Translocation of interleukin-1 $\beta$  into a vesicle intermediate in autophagy-mediated secretion. *Elife* 2015;4:e11205.
43. Chung Y, Chang SH, Martinez GJ, et al. Critical regulation of early Th17 cell differentiation by interleukin-1 signaling. *Immunity* 2009;30:576–87.
44. McGeachy MJ, Chen Y, Tato CM, et al. The interleukin 23 receptor is essential for the terminal differentiation of interleukin 17-producing effector T helper cells in vivo. *Nat Immunol* 2009;10:314–24.
45. Fujino S, Andoh A, Bamba S, et al. Increased expression of interleukin 17 in inflammatory bowel disease. *Gut* 2003;52:65–70.
46. Hueber W, Sands BE, Lewitzky S, et al.; Secukinumab in Crohn's Disease Study Group. Secukinumab, a human anti-IL-17A monoclonal antibody, for moderate to severe Crohn's disease: unexpected results of a randomised, double-blind placebo-controlled trial. *Gut* 2012;61:1693–700.
47. Ogawa A, Andoh A, Araki Y, Bamba T, Fujiyama Y. Neutralization of interleukin-17 aggravates dextran sulfate sodium-induced colitis in mice. *Clin Immunol* 2004;110:55–62.
48. Feagan BG, Sandborn WJ, Gasink C, et al.; UNIFI-IM-UNIFI Study Group. Ustekinumab as induction and maintenance therapy for Crohn's disease. *N Engl J Med* 2016;375:1946–60.
49. Yang XO, Chang SH, Park H, et al. Regulation of inflammatory responses by IL-17F. *J Exp Med* 2008;205:1063–75.
50. Hanada T, Noda NN, Satomi Y, et al. The Atg12-Atg5 conjugate has a novel E3-like activity for protein lipidation in autophagy. *J Biol Chem* 2007;282:37298–302.
51. Mizushima N, Noda T, Yoshimori T, et al. A protein conjugation system essential for autophagy. *Nature* 1998;395:395–8.
52. Noda NN, Fujioka Y, Hanada T, Ohsumi Y, Inagaki F. Structure of the Atg12-Atg5 conjugate reveals a platform for stimulating Atg8-PE conjugation. *EMBO Rep* 2013;14:206–11.
53. Sakoh-Nakatogawa M, Matoba K, Asai E, et al. Atg12-Atg5 conjugate enhances E2 activity of Atg3 by rearranging its catalytic site. *Nat Struct Mol Biol* 2013;20:433–9.
54. Chen D, Fan W, Lu Y, Ding X, Chen S, Zhong Q. A mammalian autophagosome maturation mechanism mediated by TECPR1 and the Atg12-Atg5 conjugate. *Mol Cell* 2012;45:629–41.
55. Ye X, Zhou XJ, Zhang H. Exploring the role of autophagy-related gene 5 [ATG5] yields important insights into autophagy in autoimmune/autoinflammatory diseases. *Front Immunol* 2018;9:2334.
56. Zhao Z, Fux B, Goodwin M, et al. Autophagosome-independent essential function for the autophagy protein Atg5 in cellular immunity to intracellular pathogens. *Cell Host Microbe* 2008;4:458–69.
57. Imhann F, Vich Vila A, Bonder MJ, et al. Interplay of host genetics and gut microbiota underlying the onset and clinical presentation of inflammatory bowel disease. *Gut* 2018;67:108–19.
58. Kang B, Alvarado LJ, Kim T, et al. Commensal microbiota drive the functional diversification of colon macrophages. *Mucosal Immunol* 2020;13:216–29.
59. Manichanh C, Borrueal N, Casellas F, Guarner F. The gut microbiota in IBD. *Nat Rev Gastroenterol Hepatol* 2012;9:599–608.
60. Manichanh C, Rigottier-Gois L, Bonnaud E, et al. Reduced diversity of faecal microbiota in Crohn's disease revealed by a metagenomic approach. *Gut* 2006;55:205–11.
61. Ni J, Wu GD, Albenberg L, Tomov VT. Gut microbiota and IBD: causation or correlation? *Nat Rev Gastroenterol Hepatol* 2017;14:573–84.
62. Willing BP, Dicksved J, Halfvarson J, et al. A pyrosequencing study in twins shows that gastrointestinal microbial profiles vary with inflammatory bowel disease phenotypes. *Gastroenterology* 2010;139:1844–54.e1.
63. Bain CC, Bravo-Blas A, Scott CL, et al. Constant replenishment from circulating monocytes maintains the macrophage pool in the intestine of adult mice. *Nat Immunol* 2014;15:929–37.
64. Chang PV, Hao L, Offermanns S, Medzhitov R. The microbial metabolite butyrate regulates intestinal macrophage function via histone deacetylase inhibition. *Proc Natl Acad Sci U S A* 2014;111:2247–52.
65. Mortha A, Chudnovskiy A, Hashimoto D, et al. Microbiota-dependent crosstalk between macrophages and ILC3 promotes intestinal homeostasis. *Science* 2014;343:1249288.
66. Singh N, Gurav A, Sivaprakasam S, et al. Activation of Gpr109a, receptor for niacin and the commensal metabolite butyrate, suppresses colonic inflammation and carcinogenesis. *Immunity* 2014;40:128–39.
67. Bader JE, Enos RT, Velázquez KT, et al. Macrophage depletion using clodronate liposomes decreases tumorigenesis and alters gut microbiota in the AOM/DSS mouse model of colon cancer. *Am J Physiol Gastrointest Liver Physiol* 2018;314:G22–31.
68. Niess JH, Brand S, Gu X, et al. CX3CR1-mediated dendritic cell access to the intestinal lumen and bacterial clearance. *Science* 2005;307:254–8.
69. Rescigno M, Urbano M, Valzasina B, et al. Dendritic cells express tight junction proteins and penetrate gut epithelial monolayers to sample bacteria. *Nat Immunol* 2001;2:361–7.
70. Vallon-Eberhard A, Landsman L, Yogev N, Verrier B, Jung S. Transepithelial pathogen uptake into the small intestinal lamina propria. *J Immunol* 2006;176:2465–9.
71. Seksik P. [Gut microbiota and IBD]. *Gastroenterol Clin Biol* 2010;34[Suppl 1]:S44–51.
72. Brinkman BM, Becker A, Ayiseh RB, et al. Gut microbiota affects sensitivity to acute DSS-induced colitis independently of host genotype. *Inflamm Bowel Dis* 2013;19:2560–7.
73. Roy U, Gálvez EJC, Iljazovic A, et al. Distinct microbial communities trigger colitis development upon intestinal barrier damage via innate or adaptive immune cells. *Cell Rep* 2017;21:994–1008.
74. Lee HY, Kim J, Quan W, et al. Autophagy deficiency in myeloid cells increases susceptibility to obesity-induced diabetes and experimental colitis. *Autophagy* 2016a;12:1390–403.
75. Bain CC, Schridde A. Origin, differentiation, and function of intestinal macrophages. *Front Immunol* 2018;9:2733.
76. Bain CC, Scott CL, Uronen-Hansson H, et al. Resident and pro-inflammatory macrophages in the colon represent alternative context-dependent fates of the same Ly6Chi monocyte precursors. *Mucosal Immunol* 2013;6:498–510.
77. Schridde A, Bain CC, Mayer JU, et al. Tissue-specific differentiation of colonic macrophages requires TGF $\beta$  receptor-mediated signaling. *Mucosal Immunol* 2017;10:1387–99.
78. Tamoutounour S, Henri S, Lelouard H, et al. CD64 distinguishes macrophages from dendritic cells in the gut and reveals the Th1-inducing role of mesenteric lymph node macrophages during colitis. *Eur J Immunol* 2012;42:3150–66.
79. Nakanishi Y, Sato T, Takahashi K, Ohteki T. IFN- $\gamma$ -dependent epigenetic regulation instructs colitogenic monocyte/macrophage lineage differentiation in vivo. *Mucosal Immunol* 2018;11:871–80.
80. Atarashi K, Tanoue T, Shima T, et al. Induction of colonic regulatory T cells by indigenous Clostridium species. *Science* 2011;331:337–41.
81. Chen L, Sun M, Wu W, et al. Microbiota metabolite butyrate differentially regulates Th1 and Th17 Cells' differentiation and function in induction of colitis. *Inflamm Bowel Dis* 2019;25:1450–61.
82. Ivanov II, Atarashi K, Manel N, et al. Induction of intestinal Th17 cells by segmented filamentous bacteria. *Cell* 2009;139:485–98.
83. Ivanov II, Frutos Rde L, Manel N, et al. Specific microbiota direct the differentiation of IL-17-producing T-helper cells in the mucosa of the small intestine. *Cell Host Microbe* 2008;4:337–49.

84. Sun M, Wu W, Chen L, *et al.* Microbiota-derived short-chain fatty acids promote Th1 cell IL-10 production to maintain intestinal homeostasis. *Nat Commun* 2018;9:3555.
85. Nunes NS, Kim S, Sundby M, *et al.* Temporal clinical, proteomic, histological and cellular immune responses of dextran sulfate sodium-induced acute colitis. *World J Gastroenterol* 2018;24:4341–55.
86. Ito R, Shin-Ya M, Kishida T, *et al.* Interferon-gamma is causatively involved in experimental inflammatory bowel disease in mice. *Clin Exp Immunol* 2006;146:330–8.
87. Eftychi C, Schwarzer R, Vlantis K, *et al.* Temporally distinct functions of the cytokines IL-12 and IL-23 drive chronic colon inflammation in response to intestinal barrier impairment. *Immunity* 2019;51:367–80.e4.
88. Perussia B, Chan SH, D'Andrea A, *et al.* Natural killer [NK] cell stimulatory factor or IL-12 has differential effects on the proliferation of TCR-alpha beta+, TCR-gamma delta+ T lymphocytes, and NK cells. *J Immunol* 1992;149:3495–502.
89. Trinchieri G, Wysocka M, D'Andrea A, *et al.* Natural killer cell stimulatory factor [NKSF] or interleukin-12 is a key regulator of immune response and inflammation. *Prog Growth Factor Res* 1992;4:355–68.
90. Abdi K, Singh NJ. Making many from few: IL-12p40 as a model for the combinatorial assembly of heterodimeric cytokines. *Cytokine* 2015;76:53–7.
91. Carra G, Gerosa F, Trinchieri G. Biosynthesis and posttranslational regulation of human IL-12. *J Immunol* 2000;164:4752–61.
92. D'Andrea A, Rengaraju M, Valiante NM, *et al.* Production of natural killer cell stimulatory factor [interleukin 12] by peripheral blood mononuclear cells. *J Exp Med* 1992;176:1387–98.
93. Reitberger S, Haimerl P, Aschenbrenner I, Esser-von Bieren J, Feige MJ. Assembly-induced folding regulates interleukin 12 biogenesis and secretion. *J Biol Chem* 2017;292:8073–81.
94. Harada M, Shakado S, Sakisaka S, *et al.* Bafilomycin A1, a specific inhibitor of V-type H<sup>+</sup>-ATPases, inhibits the acidification of endocytic structures and inhibits horseradish peroxidase uptake in isolated rat sinusoidal endothelial cells. *Liver* 1997;17:244–50.
95. Yoshimori T, Yamamoto A, Moriyama Y, Futai M, Tashiro Y. Bafilomycin A1, a specific inhibitor of vacuolar-type H<sup>+</sup>-ATPase, inhibits acidification and protein degradation in lysosomes of cultured cells. *J Biol Chem* 1991;266:17707–12.
96. Guo H, Chitiprolu M, Roncevic L, *et al.* Atg5 disassociates the V1V0-ATPase to promote exosome production and tumor metastasis independent of canonical macroautophagy. *Dev Cell* 2017;43:716–30.e7.
97. Peng J, Zhang R, Cui Y, *et al.* Atg5 regulates late endosome and lysosome biogenesis. *Sci China Life Sci* 2014;57:59–68.
98. Chiaruttini G, Piperno GM, Jouve M, *et al.* The SNARE VAMP7 regulates exocytic trafficking of interleukin-12 in dendritic cells. *Cell Rep* 2016;14:2624–36.
99. Cheng XT, Xie YX, Zhou B, Huang N, Farfel-Becker T, Sheng ZH. Characterization of LAMP1-labeled nondegradative lysosomal and endocytic compartments in neurons. *J Cell Biol* 2018;217:3127–39.
100. Dunster K, Toh BH, Sentry JW. Early endosomes, late endosomes, and lysosomes display distinct partitioning strategies of inheritance with similarities to Golgi-derived membranes. *Eur J Cell Biol* 2002;81:117–24.
101. Abdel Fattah E, Bhattacharya A, Herron A, Safdar Z, Eissa NT. Critical role for IL-18 in spontaneous lung inflammation caused by autophagy deficiency. *J Immunol* 2015;194:5407–16.
102. Claude-Taupin A, Bissa B, Jia J, Gu Y, Deretic V. Role of autophagy in IL-1 $\beta$  export and release from cells. *Semin Cell Dev Biol* 2018;83:36–41.
103. Kimura T, Jia J, Kumar S, *et al.* Dedicated SNAREs and specialized TRIM cargo receptors mediate secretory autophagy. *EMBO J* 2017;36:42–60.
104. Murai H, Okazaki S, Hayashi H, *et al.* Alternaria extract activates autophagy that induces IL-18 release from airway epithelial cells. *Biochem Biophys Res Commun* 2015;464:969–74.
105. Claude-Taupin A, Jia J, Mudd M, Deretic V. Autophagy's secret life: secretion instead of degradation. *Essays Biochem* 2017;61:637–47.
106. Jiang S, Dupont N, Castillo EF, Deretic V. Secretory versus degradative autophagy: unconventional secretion of inflammatory mediators. *J Innate Immun* 2013;5:471–9.
107. Mardakheh FK, Yekezare M, Machesky LM, Heath JK. Spred2 interaction with the late endosomal protein NBR1 down-regulates fibroblast growth factor receptor signaling. *J Cell Biol* 2009;187:265–77.
108. Kirkin V, Lamark T, Sou YS, *et al.* A role for NBR1 in autophagosomal degradation of ubiquitinated substrates. *Mol Cell* 2009;33:505–16.
109. Kozakov D, Hall DR, Xia B, *et al.* The ClusPro web server for protein-protein docking. *Nat Protoc* 2017;12:255–78.
110. Uhlig HH, McKenzie BS, Hue S, *et al.* Differential activity of IL-12 and IL-23 in mucosal and systemic innate immune pathology. *Immunity* 2006;25:309–18.
111. Berg DJ, Davidson N, Kühn R, *et al.* Enterocolitis and colon cancer in interleukin-10-deficient mice are associated with aberrant cytokine production and CD4<sup>+</sup> TH1-like responses. *J Clin Invest* 1996;98:1010–20.
112. Davidson NJ, Hudak SA, Lesley RE, Menon S, Leach MW, Rennick DM. IL-12, but not IFN-gamma, plays a major role in sustaining the chronic phase of colitis in IL-10-deficient mice. *J Immunol* 1998;161:3143–9.
113. Fuss IJ, Marth T, Neurath MF, Pearlstein GR, Jain A, Strober W. Anti-interleukin 12 treatment regulates apoptosis of Th1 T cells in experimental colitis in mice. *Gastroenterology* 1999;117:1078–88.
114. Neurath MF, Fuss I, Kelsall BL, Stüber E, Strober W. Antibodies to interleukin 12 abrogate established experimental colitis in mice. *J Exp Med* 1995;182:1281–90.
115. Khorrami S, Ginard D, Marín-Jiménez I, *et al.* Ustekinumab for the treatment of refractory Crohn's disease: the Spanish experience in a large multicentre open-label cohort. *Inflamm Bowel Dis* 2016;22:1662–9.
116. Mannon PJ, Fuss IJ, Mayer L, *et al.* Anti-IL-12 Crohn's Disease Study Group. Anti-interleukin-12 antibody for active Crohn's disease. *N Engl J Med* 2004;351:2069–79.
117. Sandborn WJ, Feagan BG, Fedorak RN, *et al.* Ustekinumab Crohn's Disease Study Group. A randomized trial of Ustekinumab, a human interleukin-12/23 monoclonal antibody, in patients with moderate-to-severe Crohn's disease. *Gastroenterology* 2008;135:1130–41.
118. Sandborn WJ, Gasink C, Gao LL, *et al.* CERTIFI Study Group. Ustekinumab induction and maintenance therapy in refractory Crohn's disease. *N Engl J Med* 2012;367:1519–28.
119. Wils P, Bouhnik Y, Michetti P, *et al.* Groupe d'Etude Thérapeutique des Affections Inflammatoires du Tube Digestif. Subcutaneous ustekinumab provides clinical benefit for two-thirds of patients with Crohn's disease refractory to anti-tumor necrosis factor agents. *Clin Gastroenterol Hepatol* 2016;14:242–50.e1–2.
120. Mattner F, Magram J, Ferrante J, *et al.* Genetically resistant mice lacking interleukin-12 are susceptible to infection with *Leishmania major* and mount a polarized Th2 cell response. *Eur J Immunol* 1996;26:1553–9.
121. Alpizar-Alpizar W, Laerum OD, Illemann M, *et al.* Neutrophil gelatinase-associated lipocalin [NGAL/Lcn2] is upregulated in gastric mucosa infected with *Helicobacter pylori*. *Virchows Arch* 2009;455:225–33.
122. Playford RJ, Belo A, Poulosom R, *et al.* Effects of mouse and human lipocalin homologues 24p3/lcn2 and neutrophil gelatinase-associated lipocalin on gastrointestinal mucosal integrity and repair. *Gastroenterology* 2006;131:809–17.
123. Raffatellu M, George MD, Akiyama Y, *et al.* Lipocalin-2 resistance confers an advantage to *Salmonella enterica* serotype Typhimurium for growth and survival in the inflamed intestine. *Cell Host Microbe* 2009;5:476–86.
124. Ray AL, Castillo EF, Morris KT, *et al.* Blockade of MK2 is protective in inflammation-associated colorectal cancer development. *Int J Cancer* 2016;138:770–5.
125. Inomata M, Into T, Niida S, Murakami Y. Atg5 regulates formation of MyD88 condensed structures and MyD88-dependent signal transduction. *Biochem Biophys Res Commun* 2013;437:509–14.
126. Lee HK, Mattei LM, Steinberg BE, *et al.* In vivo requirement for Atg5 in antigen presentation by dendritic cells. *Immunity* 2010;32:227–39.
127. Ndoye A, Budina-Kolomets A, Kugel CH 3rd, *et al.* ATG5 mediates a positive feedback loop between Wnt signaling and autophagy in melanoma. *Cancer Res* 2017;77:5873–85.

128. Simon HU, Yousefi S, Schmid I, Friis R. ATG5 can regulate p53 expression and activation. *Cell Death Dis* 2014;**5**:e1339.
129. Yousefi S, Perozzo R, Schmid I, et al. Calpain-mediated cleavage of Atg5 switches autophagy to apoptosis. *Nat Cell Biol* 2006;**8**:1124–32.
130. Nguyen HT, Dalmaso G, Müller S, Carrière J, Seibold F, Darfeuille-Michaud A. Crohn's disease-associated adherent invasive *Escherichia coli* modulate levels of microRNAs in intestinal epithelial cells to reduce autophagy. *Gastroenterology* 2014;**146**:508–19.
131. Cooper MA, Fehniger TA, Ponnappan A, Mehta V, Wewers MD, Caligiuri MA. Interleukin-1beta costimulates interferon-gamma production by human natural killer cells. *Eur J Immunol* 2001;**31**:792–801.
132. Tominaga K, Yoshimoto T, Torigoe K, et al. IL-12 synergizes with IL-18 or IL-1beta for IFN-gamma production from human T cells. *Int Immunol* 2000;**12**:151–60.
133. Fraser J, Simpson J, Fontana R, Kishi-Itakura C, Ktistakis NT, Gammoh N. Targeting of early endosomes by autophagy facilitates EGFR recycling and signalling. *EMBO Rep* 2019;**20**:e47734.
134. Targan SR, Feagan B, Vermeire S, et al. A randomized, double-blind, placebo-controlled phase 2 study of brodalumab in patients with moderate-to-severe Crohn's disease. *Am J Gastroenterol* 2016;**111**:1599–607.
135. Larabi A, Barnich N, Nguyen HTT. New insights into the interplay between autophagy, gut microbiota and inflammatory responses in IBD. *Autophagy* 2020;**16**:38–51.
136. Dann SM, Manthey CF, Le C, et al. IL-17A promotes protective IgA responses and expression of other potential effectors against the lumen-dwelling enteric parasite *Giardia*. *Exp Parasitol* 2015;**156**:68–78.
137. Kumar P, Monin L, Castillo P, et al. Intestinal interleukin-17 receptor signaling mediates reciprocal control of the gut microbiota and autoimmune inflammation. *Immunity* 2016;**44**:659–71.
138. Wu Y, Wang Y, Zou H, et al. Probiotic *Bacillus amyloliquefaciens* SC06 induces autophagy to protect against pathogens in macrophages. *Front Microbiol* 2017;**8**:469.
139. Lee JP, Foote A, Fan H, et al. Loss of autophagy enhances MIF/macrophage migration inhibitory factor release by macrophages. *Autophagy* 2016b;**12**:907–16.
140. Merkley SD, Chock CJ, Yang XO, Harris J, Castillo EF. Modulating T cell responses via autophagy: the intrinsic influence controlling the function of both antigen-presenting cells and T cells. *Front Immunol* 2018;**9**:2914.
141. Saitoh T, Fujita N, Jang MH, et al. Loss of the autophagy protein Atg16L1 enhances endotoxin-induced IL-1beta production. *Nature* 2008;**456**:264–8.
142. Macedo C, Turnquist HR, Castillo-Rama M, et al. Rapamycin augments human DC IL-12p70 and IL-27 secretion to promote allogeneic Type 1 polarization modulated by NK cells. *Am J Transplant* 2013;**13**:2322–33.
143. Ohtani M, Nagai S, Kondo S, et al. Mammalian target of rapamycin and glycogen synthase kinase 3 differentially regulate lipopolysaccharide-induced interleukin-12 production in dendritic cells. *Blood* 2008;**112**:635–43.
144. Said A, Bock S, Lajqi T, Müller G, Weindl G. Chloroquine promotes IL-17 production by CD4+ T cells via p38-dependent IL-23 release by monocyte-derived Langerhans-like cells. *J Immunol* 2014;**193**:6135–43.
145. Goenka MK, Kochhar R, Tandia B, Mehta SK. Chloroquine for mild to moderately active ulcerative colitis: comparison with sulfasalazine. *Am J Gastroenterol* 1996;**91**:917–21.
146. Kanvinde S, Chhonker YS, Ahmad R, et al. Pharmacokinetics and efficacy of orally administered polymeric chloroquine as macromolecular drug in the treatment of inflammatory bowel disease. *Acta Biomater* 2018;**82**:158–70.
147. Nagar J, Ranade S, Kamath V, et al. Therapeutic potential of chloroquine in a murine model of inflammatory bowel disease. *Int Immunopharmacol* 2014;**21**:328–35.
148. Park TY, Jang Y, Kim W, et al. Chloroquine modulates inflammatory autoimmune responses through Nurr1 in autoimmune diseases. *Sci Rep* 2019;**9**:15559.
149. Sands BE, Sandborn WJ, Panaccione R, et al.; UNIFI Study Group. Ustekinumab as induction and maintenance therapy for ulcerative colitis. *N Engl J Med* 2019;**381**:1201–14.
150. D'Haens G. Risks and benefits of biologic therapy for inflammatory bowel diseases. *Gut* 2007;**56**:725–32.
151. Komesu YM, Richter HE, Dinwiddie DL, et al. Methodology for a vaginal and urinary microbiome study in women with mixed urinary incontinence. *Int Urogynecol J* 2017;**28**:711–20.
152. Zhao S, Guo Y, Sheng Q, Shyr Y. Advanced heat map and clustering analysis using heatmap3. *Biomed Res Int* 2014;**2014**:986048.